# Accepted Manuscript

Experimental and modelling study of the densities of the hydrogen sulphide + methane mixtures at 253, 273 and 293 K and pressures up to 30 MPa

Alfonso Gonzalez Perez, Alain Valtz, Christophe Coquelet, Patrice Paricaud, Antonin Chapoy
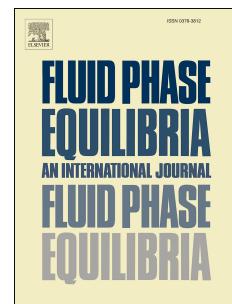
Please cite this article as: A. Gonzalez Perez, A. Valtz, C. Coquelet, P. Paricaud, A. Chapoy, Experimental and modelling study of the densities of the hydrogen sulphide + methane mixtures at 253, 273 and 293 K and pressures up to 30 MPa, *Fluid Phase Equilibria* (2016), doi: 10.1016/ j.fluid.2016.08.002.

Experimental and modelling study of the densities of the hydrogen sulphide + methane mixtures at 253, 273 and 293 K and pressures up to 30 MPa.

Alfonso Gonzalez Perez[a,b], Alain Valtz[b], Christophe Coquelet[b], Patrice Paricaud[c] and Antonin Chapoy[a,b*]

[a] *Hydrates, Flow Assurance & Phase Equilibria Research Group, Institute of Petroleum Engineering, Heriot-Watt University, Edinburgh, EH14 4AS, UK*

[b] *MINES ParisTech PSL Research University, CTP-Centre of Thermodynamics of Processes, 35 Rue Saint Honoré, 77305 Fontainebleau, France*

[c] *UCP-ENSTA ParisTech, Université Paris-Saclay, Laboratoire Chimie et Procédé, 828 Boulevard des Maréchaux, 91762 Palaiseau, France*

* Corresponding Author: Antonin Chapoy (antonin.chapoy@pet.hw.ac.uk)

ABSTRACT

Densities of three binary mixtures of hydrogen sulphide and methane (xH_2S + (1-x) CH_4), with mole fractions of 0.1315, 0.1803 and 0.2860 of acid gas, were determined experimentally at three temperatures (253, 273 and 293) K and at pressures up to 30 MPa. Densities were measured continuously using a high temperature and high pressure Vibrating Tube densitometer (VTD), Anton Paar DMA 512. The SAFT-VR Mie, PR and GERG2008 equations of state (EoS) are used to describe the experimental data with different levels of success.

Keywords: CH_4, H_2S, Thermophysical properties, Acid gas injection

1. Introduction

Many sour natural gases reservoirs and sour gas condensates fields have been discovered in the last thirty years. This kind of natural hydrocarbon gas reservoirs represent about half of the known total worldwide resources (270 trillion m^3) [1]. Acid gases are those raw natural

gases which contain significant amounts of carbon dioxide (CO_2) and hydrogen sulphide (H_2S), with compositions around of 0-80% moles CO_2 and 0-30% H_2S [2]. For this gas with high acid gas content carbon capture storage (CCS) technologies, such as oxy-fuel combustion, have the potential to become economically competitive with other zero-carbon and renewal sources of energy [3]. Thus, CCS may allow continuing to burn fossil fuels in power stations preventing CO_2 emissions to the atmosphere. CCS refers to a large number of technologies and processes, such as combustion methods (pre-combustion, post-combustion and oxy-fuel), transport pipelines or injection systems in geological basins [4]. Pressure-Volume-Temperature (PVT) data and thermophysical property models are of principal importance to the design of process involved in the capture, transport and storage of CO_2.

Since hydrogen sulphide is a toxic and corrosive compound, it is necessary to process sour gases in order to remove acid gases before their uses [5]. Different regulations require that H_2S contain of sweet gases must be less than 4 ppm. The sweetening and desulphurisation of acid gases, such as the SPREX process [6] or physical and chemical absorption with solvents, are costly processes that require accurate thermodynamic models to design natural gas processing plants. The methane-H_2S binary system is of interest to the oil and gas industry [7] because CH_4 and H_2S are important components of reservoir fluids.

There are limited references available in the literature concerning single phase density (ρ-PTx) of methane and hydrogen sulphide systems (Table 1). In 1951, Reamer et al [8] did a thorough study of this binary mixture, they were the first to measure vapour-liquid equilibria (VLE) and densities of several H_2S + CH_4 systems [9]. Reamer's density measurements cover a wide range of compositions (0.1-0.9 mol fraction H_2S), temperatures (277-411 K) and pressures (up to 69 MPa) with 1140 data. Bailey et al. [10] studied the system 49% mol of CH_4 and 51% mol of H_2S at higher temperature (501 K) The main goal of the new measurements presented in this work is to complete the literature data at low temperature.

In this paper, new density data of H_2S + CH_4 mixtures are presented for the following compositions (mole fractions): 0.1315 H_2S + 0.8685 CH_4, 0.1803 H_2S + 0.8197 CH_4 and 0.286 H_2S + 0.714 CH_4. The density of each system has been measured at three isotherms, 253, 273 and 293 K, and at pressures up to 30 MPa. The data of the three measured systems are compared to density calculations using three types of equation of state: the Peng-Robinson EoS [11], the SAFT-VR Mie EoS [12] and the multiparameter GERG-2008 EoS [13] for

natural gas). Finally, all the literature data were modelled using the three EoS proposed, in order to evaluate these models in a wider range of temperature, pressure and compositions.

2. Experimental

2.1 Sample preparation

The specification and sources of the chemicals used in this work are summarized in Table 2. Three mixtures of CH_4 and H_2S were prepared volumetrically at laboratory temperature in 300 cm^3 cylinder with its own pressure transducer to track the pressure of the sample. The final pressure target of the mixture in the vessel was approximately 40MPa in order to avoid any phase change and possible variations of composition during the injection of mixture into the densitometer set-up. To prepare the mixture, a volume of H_2S is first injected into the cylinder; thereby the injected volume will contain the number of moles calculated by an EoS to reach the expected final composition. Second, the methane is pumped in the cylinder until it the final pressure is reached. Finally, the composition of each mixture was validated by gas chromatography analysis (Varian model CP-3800). The resulting compositions of the prepared mixtures have been 0.1315, 0.1803 and 0.2860 mole fractions of H_2S.

2.2 Equipment description

A full description of the experimental set-up and procedures are available in Bouchot and Richon [14], Coquelet et al. [15] and Nazeri et al. [16]. The density of the studied mixture have been measured in a Hastelloy Vibrating Tube Densitometer (VTD), Anton Paar model DMA 512, using the one fluid reference calibration method [17].

2.3 Experimental procedure

Three isotherms of each binary system were measured at 253, 273 and 293 K. The mixture was gradually charged from the cylinder in the experimental set-up while the vibrating period, the temperature and the pressure were recorded continuously during the slow-increasing pressure up to 30 MPa and the slow decompression (the pressure in the vessel containing the mixture was maintained at pressure higher than 30 MPa during all the measurements). During the depressurisation, the acid outlet gas was neutralised by bubbling it through a column with a basic solution of sodium hydroxide.

2.4 Uncertainty of measurements

Uncertainties of the properties measured have been evaluated as standard uncertainties of type A and type B [18]. Type A of uncertainties is based on the statistical treatment of experimental data. The uncertainty of the composition measurements was evaluated as type A and it was calculated as [19]:

$$u(x_{H_2S}) = \sqrt{\frac{\sigma^2(x)}{N}}$$

(1)

where σ^2 is the variance of the values measured and N is the number of measurements. The expanded uncertainties (k=2, in order to increase the confidence level up to 95% [19]) of the composition of the three systems are 0.0006 for 0.1315 H_2S mole fraction system, 0.0008 for 0.1803 H_2S mole fraction system and 0.0011 for 0.2860 H_2S mole fraction system.

The uncertainties type B are evaluated by other means (not purely statistical), such as literature, manufacturer information, previous experience or, as in our case, calibrations. Then, uncertainty on temperature and pressure measurements was estimated as type B.

The temperature of the system in the set-up is regulated by two liquid thermoregulated baths, which temperatures are measured with two Pt100 (100Ω platinum resistance) probes. The probes calibration is done against a 25 Ω reference thermometer (Tinsley Precision Instrument). From the calibrations, the expanded uncertainty (k=2) in temperatures measurements was estimated to be 0.03 K.

The pressure was measured by two pressure transducers at two complementary ranges, one between 0-5 MPa and other from 5 up to 30 MPa. The calibration of the transducers was done using a dead weight balance (Desgranges & Huot, model 5202S). The expanded uncertainties (k=2) of the pressure measurements from the calibration are estimated to be less than 0.003 MPa for low pressure (up to 5 MPa) and 0.005 MPa for higher pressures than 5 MPa (up to 30 MPa).

Density uncertainty was evaluated as combined standard uncertainty, because density is expressed through the combination of two sources of expanded standard uncertainty: calibration and densitometer information. There is a mathematical relation ($\rho = a\tau + b$) between these standard uncertainties, therefore applying the law of propagation of uncertainty [20], density uncertainty was obtained by:

$$u(\rho) = \sqrt{\left(\frac{\partial \rho}{\partial \tau}\right)^2_{a,b} u(\tau)^2 + \left(\frac{\partial \rho}{\partial a}\right)^2_{\tau,b} u(a)^2 + \left(\frac{\partial \rho}{\partial b}\right)^2_{\tau,a} u(b)^2}$$

(2)

where τ is the vibrating period and 'a' and 'b' are the calibration parameters. From manufacturer's specifications, the standard uncertainty on the period of oscillation is 10^{-8} s. Uncertainty on the parameters of the calibration has been estimated to be 0.5% over the investigated range of pressures; however, it is worth highlighting that, due to the used technique, average uncertainty at low pressure (below 0.5 MPa) was 8.6%. The combined standard uncertainties of the measurements are reported accompanying the density data in Tables 6-14.

The calculation of the compressibility factor (Z) is function of the 3 measured properties ($Z=P/\rho RT$): temperature, pressure and density. Therefore, u(Z) gives an idea of the overall uncertainty of our experimental data because includes the uncertainty of every measurement. Then, following the same approach, the uncertainty of the Z was calculated using the law of propagation of uncertainty as:

$$u(Z) = \sqrt{\left(\frac{\partial Z}{\partial P}\right)^2_{\rho,T} u(P)^2 + \left(\frac{\partial Z}{\partial \rho}\right)^2_{P,T} u(\rho)^2 + \left(\frac{\partial Z}{\partial T}\right)^2_{P,\rho} u(T)^2}$$

(3)

Further information about calculations of the combined uncertainties of our measurements is provided in Appendix A.

3. Modelling

3.1 Peng and Robinson

The critical properties (T_c and P_c) and acentric factors (ω) of methane and hydrogen sulphide are given in Table 3. The pure component parameters have been used to model the system with the Peng and Robinson (PR) EoS [11], which is one of the most used cubic EoS due its simplicity and reasonable accuracy to correlate phase equilibria for components involved in this study such as carbon dioxide [21] or hydrogen sulphide [7]. In this work the van der Waals (classical) mixing rules are used, i.e.:

$$b = \sum_i x_i b_i$$

(4)

$$a = \sum_i \sum_j x_i x_j \sqrt{a_i a_j} \left(1 - k_{ij}\right) \tag{5}$$

where a and b are the parameters in the PR-EoS and k_{ij} the binary interaction parameter (BIP).

The BIPs are coefficients introduced to describe the experimental phase behaviour. Thus, the binary parameters avoid wrong predictions of the two phase region during density calculations. A temperature independent k_{ij} has been regressed by minimizing the objective function given in Equation 6, which is based on calculated bubble point pressures and experimental VLE data from the literature [7] [8] [22]. The regressed BIP is reported in Table 5.

$$\min \ F = \frac{100}{N} \sum_1^N \left(\frac{P_{bubble}^{\exp} - P_{bubble}^{cal}}{P_{bubble}^{\exp}} \right) \tag{6}$$

The PR-EoS tends to underestimate experimental densities [23]. Volume translations can be used in order to improve the density calculations of liquid and dense fluid phases. The Peneloux volume correction [24] has been implemented here (Equation 7) and the results with and without Peneloux shift parameters are discussed in Section 4.

$$V = V^{PR} + \sum_i^{NComp} x_i V_i^c \tag{7}$$

where V^{PR} is the molar volume calculated by the PR EoS, x_i the mole fraction of each pure component i, and V_i^c the volume correction parameter. The values of the parameters are reported in Table 3.

3.2 SAFT-VR Mie

The SAFT-VR Mie EoS proposed by Lafitte et al [12] is one of the latest updates of the SAFT family of EoS. In this equation of state, the attractive and repulsive interactions between the segments that build the molecules are described by the Mie potential that is defined as:

$$u^{Mie}(r) = \frac{\lambda_r}{\lambda_r - \lambda_a} \left(\frac{\lambda_r}{\lambda_a} \right)^{\frac{\lambda_r}{\lambda_r - \lambda_a}} \varepsilon \left(\left(\frac{\sigma}{r} \right)^{\lambda_r} - \left(\frac{\sigma}{r} \right)^{\lambda_a} \right) \tag{8}$$

where r is the intersegment distance, σ the temperature-independent segment diameter, and ε the potential depth; λ_r and λ_a are the repulsive and attractive ranges, respectively.

The SAFT-VR Mie EoS can be expressed in terms of the reduced Helmholtz energy as the sum of several contributions:

$$a = \frac{A}{nRT} = a^{IDEAL} + a^{MONOMER} + a^{CHAIN} + a^{ASSOCIATION} \tag{9}$$

The molecular parameters for CH_4 and H_2S are presented in Table 4. Hydrogen sulphide parameters were regressed using experimental saturation pressures (P_{sat}) and liquid densities (ρ_{sat}), thereby the fitting consisted in the minimization of the following objective function [12]:

$$\min_{\theta} F = \frac{1}{N_{P_{sat}}} \sum_{i=1}^{N_{P_{sat}}} \left[\frac{P_{sat,i}^{exp}(T_i) - P_{sat,i}^{calc}(T_i;\theta)}{P_{sat,i}^{exp}(T_i)} \right]^2 + \frac{1}{N_{\rho_{sat}}} \sum_{i=1}^{N_{\rho_{sat}}} \left[\frac{\rho_{sat,i}^{exp}(T_i) - \rho_{sat,i}^{calc}(T_i;\theta)}{\rho_{sat,i}^{exp}(T_i)} \right]^2 \tag{10}$$

A temperature independent binary interaction parameter was regressed following the same approach and VLE data as for the PR-EoS. The resulting k_{ij} is also reported in Table 5.

3.3 GERG

GERG-2008 is a wide-range EoS for natural gases and other similar mixtures of gases [13]. It is an empirical equation of state based on pure component EoS and correlations for the binary systems [25]. Like the SAFT EoS, GERG is expressed in terms of the Helmholtz free energy, as the sum of an ideal gas contribution and a residual part.

In this work, the PR, SAFT-VR Mie and GERG-2008 [13] EoSs were employed to predict the densities of mixtures and were implemented into the thermodynamic package HWPVT [16] [26] [27] [28] [29].

4. Result and discussion

Densities of three binary systems of CH_4 and H_2S with 0.1315, 0.1803 and 0.2860 mol fractions of hydrogen sulphide have been measured continuously using a high temperature and high pressure VTD Anton Paar. First, the densitometer calibration was done using pure ethane with a first-order polynomial calibration at 253, 273 and 293 K and pressures up to 31 MPa. Previous to the measurements, the phase envelops of the three binary systems have been studied in order to forecast at which pressure the two phase behaviour is found. The phase diagrams of the three measured systems calculated by the PR-EoS and other three systems comparing calculations against literature data [22] are shown in the Figure 1. According to Scott and van Konynenburg, the phase diagram of this system is classified as type III [7]. This

means that the curves presented in the phase envelops of Figure 1 are dew lines, therefore no density was measured in the liquid region. The studied binary mixtures are systems with no critical point [30] [31], thus all our ρ-PTx measurements have been done in the gas phase. The P-T envelops show that there is no phase change for any of the studied isotherms for the 0.1315 mol fraction of H_2S system. However, it is possible to enter the two phase region at 253K for the 0.1803 mol fraction of H_2S system and at 253 and 273K in the 0.2860 mol fraction of H_2S system.

The experimental density data for the measured systems are presented in Table 6 to Table 14. The compressibility factors derived from the measured temperature, pressure and density data, as well as their uncertainty, are also reported in the Tables 6-14.

The PR, SAFT-VR Mie and GERG-2008 equations of state have been used to model the density of the methane and hydrogen sulphide binary systems. The modelling results are presented by comparing the average deviations (%AAD) between the models and the experimental data. The AAD is the absolute average deviation and is defined as:

$$ADD \ (\%) \ = \ \frac{1}{N} \sum_{i=1}^{N} \left(\left| \rho_{\exp} \ - \ \rho_{EoS} \ \right| \middle/ \rho_{\exp} \right) \cdot 100 \tag{11}$$

The resulting SAFT-VR Mie parameters for pure hydrogen sulphide wi are reported in Table 4, as well as the AAD(%) of the equation of state from the experimental vapour pressure P_{sat}, saturated-liquid densities ρ_{sat} (Figure 2) and enthalpy of vaporization ΔH_v [32]. The pure H_2S densities in the gas, liquid and supercritical regions have been evaluated at 13 temperatures between 200 to 500 K and pressures up to 100 MPa, reporting an %AAD of 2.3%. However, considering the H_2S single phase densities at the pressure and temperature ranges of our measurements, the absolute average deviation is 0.9% (Figure 3).

BIPs for the CH_4-H_2S system have been regressed for both the SAFT-VR Mie EoS (k_{ij}=0.0314) and the PR EoS (k_{ij}=0.0807) models using VLE data from the literature [7] [8] [22] (Figure 4). Using these BIPs, the PR EoS is slightly more accurate to correlate the phase behaviour of the CH_4-H_2S system than the SAFT-VR Mie EoS, with bubble point pressure AADs of 4.4% and 4.8%, respectively.

The deviations of the PR, SAFT-VR Mie and GERG-2008 models for the three measured systems at each temperature are reported in Table 15. Generally, the SAFT-VR Mie EoS

shows lower overall deviations (AAD=2.5%) than the other two models, PR EoS (3.0%) and GERG-2008 (3.4%). The experimental densities measured in this work and the predicted densities for the system 0.2860 H_2S mol fraction systems by using the GERG-2008 and SAFT-VR Mie are illustrated in Figures 5. As the GERG EoS is an empirical model developed for natural gases whose parameters for the CH_4+H_2S binary system have been fitted to experimental data over wide ranges of temperature (189 to 501 K), pressure (0.048 to 68.9 MPa) and methane mol fraction (0.1 to 0.9993) [13], it was unexpected that the GERG-2008 EoS reported the highest deviations for these systems, particularly for the 0.2860 mol fraction of H_2S system (Figure 5) with an AAD of 4.9%. However, the GERG-2008 EoS presents better results than SAFT and PR EoSs for the binary mixture with smaller amount of H_2S.

Density data available in the literature (1748 points) and those measured in this work have been modelled with the PR, PR + Peneloux volume correction, SAFT-VR Mie and GERG-2008 equations of state, and the deviations are listed in Table 16. As can be observed, the SAFT-VR Mie EoS reports the lower deviation between experimental and calculated densities with an AAD of 4.3%, while GERG-2008 shows similar level of agreement (4.6%). The experimental densities of 50 mol% H_2S + 50 mol% CH_4 and the predicted densities using the PR + Peneloux, GERG-2008 and SAFT-VR Mie EoSs are presented in Figure 6, as an example of the modelling result of this system at high pressure (up to 70MPa).

The PR-EoS is the studied model that has reported the largest total deviation (AAD=7.8%), especially when PR calculations are compared against Reamer et al. [8] data at pressures over 30 MPa. The results of the PR –EoS with volume correction (VC) have not been presented in Table 6 because no better density predictions were observed after applying the Peneloux VC to model our measured densities. However, remarkable improvements in the density calculations with the PR-EoS can be noticed in the results of modelling the full Reamer's data set using the PR-Peneloux, decreasing by half the ADD. The AAD reduces from 7.8% to 5.4% when the complete density data set is modelled using the PR with Peneloux shift model. Figure 7 shows the comparison of PR and PR-Peneloux calculations against literature data of the 0.3 mol fraction H_2S system, in order to illustrate the large deviations of PR EoS at high pressure.

The uncertainties for each measured density are reported in Tables 6-14. The uncertainties were evaluated as combined standard uncertainty with 95% level of confidence. Despite the

low average uncertainty (0.5%), the uncertainty of the density measurements below 0.5MPa is 8.3% with a maximum value of 10.1%. This high uncertainty was expected due to the fact that the vibrating tube densitometer is not the most appropriate technique for the determination of the densities of gases at low pressure (i.e. low mass in the VTD) [33]. The elevated uncertainty of density at low pressure is propagated to compressibility factor calculations (Figure 8).

The volumetric behaviour of the $CH_4 + H_2S$ binary mixture at low pressure has been studied with the virial expansion truncated after the second coefficient. A virial equation provides a simple way to describe thermodynamic properties, and the virial coefficients can be determined by different experimental methods or correlations [34]. The form for our virial expansion is given by:

$$Z = 1 + \rho\, B(T, x_1)$$
(12)

where B is the second virial coefficient which is calculated as a function of temperature and mol fraction of methane (x_1) as:

$$B(T, x_1) = a + \frac{b}{T} + \frac{c}{T^3} + d x_1$$
(13)

where a, b, c and d are the parameters reported in Table 17. These parameters have been correlated using our density measurements and the low pressure $\rho\text{-}PTx$ data sets from the literature [8] [10]. The correlated virial equation of state has an AAD of 1.5% with a maximum deviation of 5.7% in a wide range of compositions, pressures up to 1.9 MPa and temperatures between 253 and 500 K (Figure 9). Several isotherms calculated with our CH_4+H_2S virial equation of state are illustrated in Figure 10.

5. Conclusion

Density data measurements for the three binary mixtures of methane with 0.1315, 0.1803 and 0.286 mol fraction of hydrogen sulphide were performed at three temperatures between 253 and 293 K and pressures up to 30 MPa by using a vibrating tube Anton Paar densitometer. The average uncertainty of the measurements at the 95% confidence level is 0.5%, reporting the highest average uncertainty of 8.3% at low pressures (below 0.5 MPa).

The measured experimental data were compared with the densities predicted with the PR, SAFT-VR Mie and GERG-2008 equations of state. For these measurements the SAFT-VR Mie EoS has the lowest absolute average deviation (2.5%) among the three investigated models. However deviations for all models are of the same order (3.4 % for the GERG EoS and for 3.0 % the PR EoS without volume correction 3.0%). However, theGERG-2008 is slightly superior to describe the density of the 0.1315 mol fraction of H_2S system (AAD=2.8%) than the SAFT-VR Mie (AAD=3.0%) and PR (AAD=2.9%) EoSs.

Furthermore, the literature data have been studied with the different models. When compared against the full density dataset, the lowest deviations are observed for the SAFT-VR Mie (4.3 %). The deviations with GERG-2008, PR, PR-Peneloux EoSs were 4.6, 7.8 and 5.4 %, respectively. Significant improvement in density predictions are observed when volume correction are used with the PR-EoS, due to the overestimated densities predicted by the PR EoS at pressures over 30MPa.

Finally, the measured densities and the ρ-PTx data from the literature at low pressure were used to correlate the second virial coefficient as a function of temperature and CH_4 mol fraction. The absolute average deviation of the compressibility factor calculated from our virial EoS in a wide range of compositions and at pressures up to 1.9 MPa and temperatures between 253 and 500 K is 1.5% with a maximum deviation of 5.7%.

Appendix A. Uncertainty in density measurements and compressibility factors

Density uncertainty was evaluated as combined standard uncertainty [18] [20]. Density measurement uncertainty can be expressed through the combination of two sources of expanded standard uncertainty, calibration and densitometer information, due to the mathematical relation used to do the calibration:

$$\rho = a\tau + b \tag{A1}$$

Therefore, applying the law of propagation of uncertainty [20], density uncertainty was obtained by:

$$u(\rho) = \sqrt{\left(\frac{\partial\rho}{\partial\tau}\right)_{a,b}^2 u(\tau)^2 + \left(\frac{\partial\rho}{\partial a}\right)_{\tau,b}^2 u(a)^2 + \left(\frac{\partial\rho}{\partial b}\right)_{\tau,a}^2 u(b)^2} \tag{A2}$$

where τ is the time of oscillation and both 'a' and 'b' are the calibration parameters. Subsequently, the partial derivatives required for calculating $u(\rho)$ are derived from equation A1 as:

$$\left(\frac{\partial\rho}{\partial\tau}\right)_{a,b} = a \qquad\qquad \left(\frac{\partial\rho}{\partial a}\right)_{\tau,b} = \tau \qquad\qquad \left(\frac{\partial\rho}{\partial b}\right)_{a,\tau} = 1 \tag{A3}$$

Finally, the combined standard uncertainty of our density measurements can be expressed by

$$u(\rho) = \sqrt{a^2 u(\tau)^2 + \tau^2 u(a)^2 + u(b)^2}, \tag{A4}$$

u(a) and u(b) are the standard deviations calculated after linear regression between reference fluid density values and measured period of vibration at the corresponding temperature of calibration. The calculation of the compressibility factor (Z) is function of the 3 properties measured: temperature, pressure and density. The compressibility factor can be formulated as

$$Z = \frac{P}{\rho R T} \tag{A5}$$

Consequently, uncertainty in compressibility factor calculation, $u(Z)$, gives an idea of the overall uncertainty of our experimental data due to the consideration of the uncertainties of every measurement. Thus, following the same approach for the propagation of the uncertainty, the uncertainties of the compressibility factors were calculated using the law of propagation as:

$$u(Z) = \sqrt{\left(\frac{\partial Z}{\partial P}\right)_{\rho,T}^2 u(P)^2 + \left(\frac{\partial Z}{\partial \rho}\right)_{P,T}^2 u(\rho)^2 + \left(\frac{\partial Z}{\partial T}\right)_{P,\rho}^2 u(T)^2} \tag{A6}$$

where the partial derivatives are obtained from deriving the equation A5 as follows:

$$\left(\frac{\partial Z}{\partial P}\right)_{\rho,T} = \frac{1}{\rho R T} \qquad\qquad \left(\frac{\partial Z}{\partial \rho}\right)_{P,T} = -\frac{P}{\rho^2 R T} \qquad\qquad \left(\frac{\partial Z}{\partial T}\right)_{\rho,P} = -\frac{P}{\rho R T^2} \tag{A7}$$

Table 1 - Available experimental ρ-PTx data in the literature with their uncertainties for the methane and hydrogen sulphide system.

Reference	Year	No of Data	H$_2$S mol fraction		Pressure		Temperature		Density	
			Range (%)	u(x_{H2S}) (%)	Range (MPa)	u(P) (MPa)	Range (K)	u(T) (K)	Range (kg$\cdot$m^{-3})	u(P) (%)
Reamer et al. [8]	1951	1140	10-90	0.3	1-69	0.001	277-411	0.01	1-69	0.5
Bailey et al. [10]	1987	80	50.7	0.01	0.2-38	0.003	299-501	0.01	1-230	1

Table 2 - Details of the chemicals, suppliers and purities of the components used in this study.

Chemical Name	Source	Initial Purity [a]	Certification	Analysis Method [b]
Hydrogen sulphide	Air Liquide	0.995 vol	Air Liquide Certified	SM
Methane	Air Liquide	0.99995 vol	Air Liquide Certified	SM

[a] No additional purification is carried out.
[b] SM: Supplier method

Table 3 - Critical parameters, acentric factors and volume correction parameters for methane and hydrogen sulphide.

Compound	T_c/K	P_c/MPa	ω	V^C_i/ $m^3 \cdot m^{-1}$
CH_4	190.58	4.604	0.01083	-5.02
H_2S	373.20	8.963	0.081	-4.02

Table 4 –Mie molecular parameters for pure methane and hydrogen sulphide, and average absolute deviation (%AAD)from pure experimental data [32] for the vapour pressure (P_{sat}), the saturated-liquid density (ρ_{sat}) and the enthalpy of vaporization (ΔH_v).

Compound	m_s	$\sigma/\text{Å}$	$(\varepsilon/k)/K$	λ_r	λ_a	AAD (%)		
						P_{sat}	ρ_{sat}	ΔH_v
H_2S (this work)	1	3.7783	387.28	22.451	6	2.2	0.4	3.7
CH_4 [12]	1	3.7412	153.36	12.650	6	0.7	0.8	2.9

Table 5 - Regressed k_{ij} values for PR and SAFT-VR Mie EoSs and their absolute average deviations (%AAD) in bubble point pressure and vapour phase composition calculations for the methane + hydrogen sulphide binary system.

	k_{ij}	%AAD P^{bubble}	%AAD y_1
PR	0.0807	4.4	1.9
SAFT-VR Mie	0.0314	4.8	2.0

Table 6 – Experimental results of the 0.8685 mole CH$_4$ + 0.1315 mole H$_2$S system at 253K, u(x$_{H2S}$)= 0.0006, u(T)= 0.03 K, u(P)= 0.003 MPa for pressures up to 5 MPa and u(P)= 0.005 MPa for pressures from 5 to 30 MPa.

No	T	P	ρ	u(ρ)		Z	u(Z)	No	T	P	ρ	u(ρ)		Z	u(Z)
	[K]	[MPa]	$\left[\dfrac{kg}{m^3}\right]$	$\left[\dfrac{kg}{m^3}\right]$	%		10^{-2}		[K]	[MPa]	$\left[\dfrac{kg}{m^3}\right]$	$\left[\dfrac{kg}{m^3}\right]$	%		10^{-2}
1	253.28	0.188	1.76	0.18	10.1	0.93	9.4	37	253.46	12.710	199.55	1.00	0.5	0.56	0.3
2	253.29	0.508	4.80	0.22	4.7	0.92	4.3	38	253.47	13.026	204.72	1.03	0.5	0.56	0.3
3	253.30	1.250	12.25	0.33	2.7	0.89	2.4	39	253.48	13.361	209.99	1.06	0.5	0.56	0.3
4	253.31	1.824	18.07	0.41	2.3	0.88	2.0	40	253.49	13.557	213.18	1.07	0.5	0.56	0.3
5	253.33	2.475	24.75	0.50	2.0	0.87	1.8	41	253.50	13.904	217.77	1.10	0.5	0.56	0.3
6	253.35	3.335	33.57	0.52	1.5	0.87	1.3	42	253.53	14.217	222.31	1.13	0.5	0.56	0.3
7	253.36	4.114	41.57	0.54	1.3	0.87	1.1	43	253.53	14.605	227.86	1.16	0.5	0.56	0.3
8	253.38	4.487	45.79	0.55	1.2	0.86	1.0	44	253.54	15.328	236.23	1.23	0.5	0.57	0.3
9	253.34	4.807	49.57	0.56	1.1	0.85	1.0	45	253.56	16.209	246.09	1.31	0.5	0.58	0.3
10	253.33	5.174	53.92	0.57	1.1	0.84	0.9	46	253.58	16.612	250.04	1.33	0.5	0.58	0.3
11	253.32	5.258	55.98	0.58	1.0	0.82	0.8	47	253.59	17.129	255.23	1.26	0.5	0.59	0.3
12	253.33	5.895	64.88	0.60	0.9	0.79	0.7	48	253.60	17.589	259.35	1.21	0.5	0.59	0.3
13	253.32	6.503	73.25	0.62	0.9	0.78	0.7	49	253.61	18.036	263.28	1.15	0.4	0.60	0.3
14	253.34	6.994	80.75	0.65	0.8	0.76	0.6	50	253.61	18.480	267.15	1.10	0.4	0.60	0.2
15	253.36	7.255	84.54	0.66	0.8	0.75	0.6	51	253.62	18.822	269.80	1.06	0.4	0.61	0.2
16	253.35	7.572	90.00	0.67	0.7	0.74	0.6	52	253.63	19.390	274.47	1.00	0.4	0.62	0.2
17	253.35	7.961	99.59	0.69	0.7	0.70	0.5	53	253.64	19.853	277.53	0.96	0.3	0.63	0.2
18	253.36	8.383	108.50	0.72	0.7	0.68	0.4	54	253.66	21.081	286.30	0.84	0.3	0.64	0.2
19	253.37	8.539	112.16	0.72	0.6	0.67	0.4	55	253.66	21.605	289.87	0.80	0.3	0.65	0.2
20	253.38	8.660	115.11	0.73	0.6	0.66	0.4	56	253.67	22.087	292.82	0.76	0.3	0.66	0.2
21	253.38	8.850	119.77	0.74	0.6	0.65	0.4	57	253.68	22.512	295.31	0.73	0.2	0.67	0.2
22	253.39	9.030	124.20	0.75	0.6	0.64	0.4	58	253.68	22.918	297.52	0.70	0.2	0.67	0.2
23	253.40	9.215	128.92	0.76	0.6	0.63	0.4	59	253.56	23.487	300.68	0.66	0.2	0.68	0.2
24	253.40	9.484	135.48	0.78	0.6	0.61	0.4	60	253.29	24.245	303.67	0.62	0.2	0.70	0.1
25	253.43	9.711	140.67	0.79	0.6	0.60	0.3	61	253.29	24.733	306.89	0.59	0.2	0.70	0.1
26	253.43	9.944	145.46	0.81	0.6	0.60	0.3	62	253.30	25.670	310.08	0.55	0.2	0.72	0.1
27	253.41	10.167	150.17	0.82	0.5	0.59	0.3	63	253.57	26.154	313.25	0.53	0.2	0.73	0.1
28	253.42	10.405	155.11	0.84	0.5	0.59	0.3	64	253.72	26.573	314.90	0.51	0.2	0.74	0.1
29	253.44	10.674	160.71	0.85	0.5	0.58	0.3	65	253.53	27.036	316.40	0.50	0.2	0.75	0.1
30	253.42	10.879	164.94	0.87	0.5	0.58	0.3	66	253.32	27.359	317.71	0.49	0.2	0.75	0.1
31	253.42	11.161	170.62	0.89	0.5	0.57	0.3	67	253.32	27.986	320.59	0.48	0.1	0.76	0.1
32	253.45	11.408	175.60	0.90	0.5	0.57	0.3	68	253.33	28.601	322.89	0.47	0.1	0.77	0.1
33	253.46	11.691	181.06	0.93	0.5	0.56	0.3	69	253.33	29.015	324.42	0.46	0.1	0.78	0.1
34	253.46	11.951	186.09	0.94	0.5	0.56	0.3	70	253.31	29.542	326.32	0.46	0.1	0.79	0.1
35	253.46	12.221	190.99	0.96	0.5	0.56	0.3	71	253.33	30.002	327.17	0.46	0.1	0.80	0.1
36	253.45	12.503	195.90	0.99	0.5	0.56	0.3								

Table 7 – Experimental results of the 0.8685 mole CH$_4$ + 0.1315 mole H$_2$S system at 273K, u(x$_{H2S}$)= 0.0006, u(T)= 0.03 K, u(P)= 0.003 MPa for pressures up to 5 MPa and u(P)=0.005 MPa for pressures from 5 to 30 MPa.

No	T	P	ρ	u(ρ)		Z	u(Z)	No	T	P	ρ	u(ρ)		Z	u(Z)
	[K]	[MPa]	$\left[\dfrac{kg}{m^3}\right]$	$\left[\dfrac{kg}{m^3}\right]$	%		10^{-2}		[K]	[MPa]	$\left[\dfrac{kg}{m^3}\right]$	$\left[\dfrac{kg}{m^3}\right]$	%		10^{-2}
1	273.21	0.209	1.70	0.17	10.0	0.99	9.6	31	273.26	11.726	146.08	0.69	0.5	0.65	0.3
2	273.21	0.648	5.39	0.22	4.1	0.97	4.0	32	273.26	12.002	150.33	0.70	0.5	0.65	0.3
3	273.24	1.167	10.00	0.26	2.6	0.95	2.5	33	273.26	12.322	155.19	0.72	0.5	0.64	0.3
4	273.24	1.761	15.44	0.30	2.0	0.92	1.8	34	273.26	12.637	159.86	0.74	0.5	0.64	0.3
5	273.25	2.240	19.97	0.34	1.7	0.91	1.5	35	273.26	13.040	165.72	0.76	0.5	0.64	0.3
6	273.26	2.770	25.12	0.37	1.5	0.89	1.3	36	273.27	13.466	171.70	0.78	0.5	0.64	0.3
7	273.27	3.280	30.25	0.40	1.3	0.88	1.1	37	273.27	13.771	175.85	0.80	0.5	0.64	0.3
8	273.25	3.776	35.41	0.42	1.2	0.86	1.0	38	273.30	14.847	189.62	0.87	0.5	0.63	0.3
9	273.27	4.207	40.03	0.44	1.1	0.85	0.9	39	273.31	15.329	195.37	0.90	0.5	0.64	0.3
10	273.27	4.225	40.23	0.44	1.1	0.85	0.9	40	273.32	15.811	200.85	0.93	0.5	0.64	0.3
11	273.26	4.666	45.13	0.45	1.0	0.84	0.8	41	273.32	16.120	204.24	0.96	0.5	0.64	0.3
12	273.26	5.086	49.93	0.47	0.9	0.83	0.8	42	273.32	16.817	211.55	1.00	0.5	0.64	0.3
13	273.28	5.512	54.98	0.48	0.9	0.81	0.7	43	273.33	17.352	216.85	1.04	0.5	0.65	0.3
14	273.28	5.933	60.12	0.48	0.8	0.80	0.6	44	273.34	17.978	222.75	1.09	0.5	0.65	0.3
15	273.30	6.333	65.17	0.49	0.8	0.79	0.6	45	273.34	18.233	225.06	1.11	0.5	0.66	0.3
16	273.31	6.712	70.10	0.51	0.7	0.78	0.6	46	273.35	18.773	229.81	1.05	0.5	0.66	0.3
17	273.31	7.200	76.68	0.52	0.7	0.76	0.5	47	273.35	19.531	236.12	0.97	0.4	0.67	0.3
18	273.31	7.483	80.60	0.52	0.6	0.75	0.5	48	273.37	20.048	240.23	0.83	0.3	0.68	0.2
19	273.31	7.817	85.33	0.53	0.6	0.74	0.5	49	273.36	20.692	245.12	0.68	0.3	0.68	0.2
20	273.29	8.136	89.96	0.54	0.6	0.73	0.4	50	273.33	21.405	250.29	0.54	0.2	0.69	0.1
21	273.28	8.496	95.31	0.55	0.6	0.72	0.4	51	273.31	22.905	260.37	0.36	0.1	0.71	0.1
22	273.29	8.809	100.05	0.56	0.6	0.71	0.4	52	273.29	23.690	265.29	0.34	0.1	0.72	0.1
23	273.27	9.149	105.29	0.57	0.5	0.70	0.4	53	273.27	24.569	270.52	0.31	0.1	0.74	0.1
24	273.28	9.596	112.28	0.59	0.5	0.69	0.4	54	273.27	25.361	275.02	0.29	0.1	0.75	0.1
25	273.27	9.851	116.33	0.60	0.5	0.69	0.4	55	273.27	26.319	280.21	0.26	0.1	0.76	0.1
26	273.28	10.137	120.88	0.61	0.5	0.68	0.3	56	273.26	27.255	285.03	0.24	0.1	0.77	0.1
27	273.29	10.446	125.82	0.63	0.5	0.67	0.3	57	273.26	28.276	290.05	0.23	0.1	0.79	0.1
28	273.29	10.749	130.66	0.64	0.5	0.67	0.3	58	273.26	29.372	295.19	0.21	0.1	0.81	0.1
29	273.26	11.062	135.65	0.65	0.5	0.66	0.3	59	273.25	30.481	300.13	0.21	0.1	0.82	0.1
30	273.25	11.361	140.37	0.67	0.5	0.66	0.3								

Table 8 – Experimental results of the 0.8685 mole CH$_4$ + 0.1315 mole H$_2$S system at 293K, u(x$_{H2S}$)= 0.0006, u(T)= 0.03 K, u(P)= 0.003 MPa for pressures up to 5 MPa and u(P)= 0.005 MPa for pressures from 5 to 30 MPa.

No	T	P	ρ	u(ρ)		Z	u(Z)	No	T	P	ρ	u(ρ)		Z	u(Z)
	[K]	[MPa]	$\left[\frac{kg}{m^3}\right]$	$\left[\frac{kg}{m^3}\right]$	%		10^{-2}		[K]	[MPa]	$\left[\frac{kg}{m^3}\right]$	$\left[\frac{kg}{m^3}\right]$	%		10^{-2}
1	293.18	0.239	1.86	0.18	9.5	0.97	9.2	31	293.19	13.230	140.02	0.71	0.5	0.71	0.4
2	293.18	0.469	3.71	0.19	5.3	0.96	5.0	32	293.18	13.726	145.96	0.74	0.5	0.71	0.4
3	293.19	0.792	6.46	0.22	3.4	0.93	3.2	33	293.20	14.242	152.42	0.76	0.5	0.71	0.4
4	293.21	1.117	9.20	0.24	2.7	0.92	2.4	34	293.20	14.579	156.48	0.78	0.5	0.70	0.4
5	293.19	1.341	11.22	0.26	2.3	0.90	2.1	35	293.20	14.924	160.62	0.81	0.5	0.70	0.4
6	293.20	1.820	15.41	0.29	1.9	0.89	1.7	36	293.20	15.365	165.51	0.83	0.5	0.70	0.4
7	293.19	2.300	20.14	0.32	1.6	0.86	1.4	37	293.20	15.806	170.31	0.86	0.5	0.70	0.4
8	293.18	2.890	25.81	0.36	1.4	0.85	1.2	38	293.19	16.228	174.96	0.89	0.5	0.70	0.4
9	293.19	3.396	30.35	0.38	1.3	0.85	1.1	39	293.19	16.699	180.07	0.92	0.5	0.70	0.4
10	293.19	3.988	35.82	0.41	1.1	0.84	1.0	40	293.20	17.183	185.14	0.95	0.5	0.70	0.4
11	293.19	4.428	40.25	0.42	1.0	0.83	0.9	41	293.19	17.682	190.29	0.98	0.5	0.70	0.4
12	293.20	4.887	44.78	0.44	1.0	0.82	0.8	42	293.20	18.163	195.16	1.01	0.5	0.70	0.4
13	293.20	5.494	50.99	0.45	0.9	0.81	0.7	43	293.23	18.686	200.27	0.99	0.5	0.71	0.3
14	293.20	5.964	55.59	0.46	0.8	0.81	0.7	44	293.29	19.219	205.31	0.87	0.4	0.71	0.3
15	293.20	6.411	60.21	0.46	0.8	0.80	0.6	45	293.23	19.770	210.30	0.73	0.3	0.71	0.2
16	293.19	6.909	65.40	0.47	0.7	0.80	0.6	46	293.22	20.355	215.54	0.58	0.3	0.71	0.2
17	293.19	7.335	70.05	0.48	0.7	0.79	0.5	47	293.20	20.932	220.42	0.43	0.2	0.72	0.1
18	293.19	7.786	74.96	0.49	0.7	0.79	0.5	48	293.20	21.495	224.99	0.39	0.2	0.72	0.1
19	293.18	8.263	79.99	0.50	0.6	0.78	0.5	49	293.23	22.173	230.34	0.37	0.2	0.73	0.1
20	293.18	8.722	85.68	0.51	0.6	0.77	0.5	50	293.23	22.860	235.56	0.34	0.1	0.73	0.1
21	293.19	9.097	90.09	0.53	0.6	0.76	0.4	51	293.21	23.505	240.20	0.32	0.1	0.74	0.1
22	293.19	9.534	95.16	0.54	0.6	0.76	0.4	52	293.22	24.254	245.19	0.30	0.1	0.75	0.1
23	293.18	9.972	100.39	0.56	0.6	0.75	0.4	53	293.22	25.052	250.52	0.28	0.1	0.76	0.1
24	293.19	10.368	105.20	0.57	0.5	0.74	0.4	54	293.21	25.865	255.77	0.26	0.1	0.76	0.1
25	293.19	10.794	110.28	0.59	0.5	0.74	0.4	55	293.21	26.669	260.49	0.24	0.1	0.77	0.1
26	293.19	11.183	115.06	0.61	0.5	0.73	0.4	56	293.20	27.629	265.96	0.22	0.1	0.79	0.1
27	293.19	11.608	120.16	0.63	0.5	0.73	0.4	57	293.20	28.496	270.59	0.21	0.1	0.80	0.1
28	293.18	12.003	124.94	0.65	0.5	0.73	0.4	58	293.21	29.415	275.27	0.20	0.1	0.81	0.1
29	293.18	12.415	130.08	0.67	0.5	0.72	0.4	59	293.21	29.995	278.16	0.20	0.1	0.81	0.1
30	293.18	12.830	135.13	0.69	0.5	0.72	0.4	60	293.21	30.419	280.17	0.19	0.1	0.82	0.1

Table 9 – Experimental results of 0.8197 mole CH$_4$ + 0.1803 mole H$_2$S system at 253K, u(x$_{H2S}$)= 0.0008, u(T)= 0.03 K, u(P)= 0.003 MPa for pressures up to 5 MPa and u(P)= 0.005 MPa for pressures from 5 to 30 MPa.

No	T	P	ρ	u(ρ)		Z	u(Z)	No	T	P	ρ	u(ρ)		Z	u(Z)
	[K]	[MPa]	$\left[\dfrac{kg}{m^3}\right]$	$\left[\dfrac{kg}{m^3}\right]$	%		10^{-2}		[K]	[MPa]	$\left[\dfrac{kg}{m^3}\right]$	$\left[\dfrac{kg}{m^3}\right]$	%		10^{-2}
1	253.03	0.225	2.10	0.18	8.7	0.98	8.6	31	252.98	16.314	285.18	1.32	0.5	0.53	0.2
2	253.05	0.472	4.43	0.22	4.9	0.97	4.8	32	252.99	16.702	288.37	1.32	0.5	0.53	0.2
3	253.07	1.105	10.58	0.31	2.9	0.96	2.8	33	253.01	17.275	293.02	1.24	0.4	0.54	0.2
4	253.08	1.496	14.53	0.36	2.5	0.94	2.4	34	253.02	17.701	296.11	1.19	0.4	0.55	0.2
5	253.08	2.006	20.39	0.43	2.1	0.90	1.9	35	253.03	18.070	299.00	1.15	0.4	0.55	0.2
6	253.25	2.607	28.21	0.50	1.8	0.85	1.5	36	253.02	18.537	302.29	1.10	0.4	0.56	0.2
7	253.21	2.947	32.50	0.51	1.6	0.83	1.3	37	253.02	19.009	305.49	1.04	0.3	0.57	0.2
8	253.16	3.517	38.95	0.52	1.3	0.83	1.1	38	253.02	19.564	309.06	0.99	0.3	0.58	0.2
9	253.19	4.054	46.42	0.54	1.2	0.80	0.9	39	253.01	20.084	312.27	0.93	0.3	0.59	0.2
10	253.18	4.507	52.31	0.55	1.1	0.79	0.8	40	253.01	20.574	315.19	0.89	0.3	0.60	0.2
11	253.12	4.809	59.33	0.56	0.9	0.74	0.7	41	253.00	21.010	317.91	0.85	0.3	0.61	0.2
12	253.13	5.304	67.27	0.58	0.9	0.72	0.6	42	253.00	21.473	320.52	0.81	0.3	0.61	0.2
13	252.91	9.089	146.00	0.75	0.5	0.57	0.3	43	253.00	21.973	323.20	0.77	0.2	0.62	0.1
14	252.91	9.296	153.90	0.77	0.5	0.55	0.3	44	253.00	22.531	326.01	0.73	0.2	0.63	0.1
15	252.91	9.508	162.60	0.78	0.5	0.54	0.3	45	253.00	22.822	327.46	0.71	0.2	0.64	0.1
16	252.91	9.727	172.12	0.79	0.5	0.52	0.2	46	253.00	23.125	329.05	0.69	0.2	0.64	0.1
17	252.90	9.948	181.75	0.81	0.4	0.50	0.2	47	253.01	23.774	332.07	0.64	0.2	0.66	0.1
18	252.90	10.181	191.68	0.82	0.4	0.49	0.2	48	253.01	24.145	333.77	0.62	0.2	0.66	0.1
19	252.90	10.440	200.58	0.84	0.4	0.48	0.2	49	253.02	24.553	335.64	0.60	0.2	0.67	0.1
20	252.89	10.727	209.51	0.86	0.4	0.47	0.2	50	253.02	25.031	337.77	0.58	0.2	0.68	0.1
21	252.89	11.063	217.25	0.88	0.4	0.47	0.2	51	253.03	25.582	340.15	0.55	0.2	0.69	0.1
22	252.89	11.429	224.63	0.91	0.4	0.47	0.2	52	253.04	26.249	342.94	0.52	0.2	0.70	0.1
23	252.90	11.825	231.88	0.93	0.4	0.47	0.2	53	253.07	26.760	345.19	0.51	0.1	0.71	0.1
24	252.90	12.251	239.02	0.97	0.4	0.47	0.2	54	253.07	27.152	346.63	0.50	0.1	0.72	0.1
25	252.91	12.717	246.10	1.00	0.4	0.47	0.2	55	253.06	27.510	348.27	0.49	0.1	0.72	0.1
26	252.92	13.223	253.09	1.04	0.4	0.48	0.2	56	253.07	28.062	350.41	0.48	0.1	0.73	0.1
27	252.92	13.782	260.02	1.09	0.4	0.49	0.2	57	253.08	28.543	352.25	0.47	0.1	0.74	0.1
28	252.94	14.392	266.89	1.14	0.4	0.50	0.2	58	253.08	28.966	353.85	0.46	0.1	0.75	0.1
29	252.95	15.070	273.89	1.20	0.4	0.51	0.2	59	253.08	29.496	355.79	0.46	0.1	0.76	0.1
30	252.97	15.829	280.91	1.28	0.5	0.52	0.2	60	253.08	30.039	357.73	0.46	0.1	0.77	0.1

Table 10 – Experimental results of the 0.8197 mole CH$_4$ + 0.1803 mole H$_2$S system at 273K, u(x$_{H2S}$)= 0.0008, u(T)= 0.03 K, u(P)= 0.003 MPa for pressures up to 5 MPa and u(P)=0.005 MPa for pressures from 5 to 30 MPa.

No	T [K]	P [MPa]	ρ $\left[\dfrac{kg}{m^3}\right]$	u(ρ) $\left[\dfrac{kg}{m^3}\right]$	u(ρ) %	Z	u(Z) 10^{-2}	No	T [K]	P [MPa]	ρ $\left[\dfrac{kg}{m^3}\right]$	u(ρ) $\left[\dfrac{kg}{m^3}\right]$	u(ρ) %	Z	u(Z) 10^{-2}
1	273.04	0.220	1.87	0.18	9.6	1.00	9.5	32	273.13	15.510	224.73	0.91	0.4	0.59	0.2
2	273.05	0.512	4.39	0.21	4.8	0.99	4.6	33	273.13	16.041	231.85	0.95	0.4	0.59	0.2
3	273.06	1.024	8.86	0.25	2.8	0.98	2.3	34	273.13	16.504	237.74	0.98	0.4	0.59	0.2
4	273.06	1.546	13.54	0.29	2.1	0.97	2.0	35	273.11	17.004	243.74	1.02	0.4	0.59	0.2
5	273.06	1.998	17.83	0.32	1.8	0.95	1.7	36	273.08	17.522	249.57	1.06	0.4	0.60	0.2
6	273.07	2.472	22.64	0.35	1.5	0.93	1.4	37	273.10	18.017	254.80	1.09	0.4	0.60	0.2
7	273.08	3.006	28.12	0.38	1.4	0.91	1.2	38	273.08	18.504	259.61	1.13	0.4	0.61	0.2
8	273.08	3.496	33.34	0.41	1.2	0.89	1.1	39	273.07	19.004	264.22	1.12	0.4	0.61	0.2
9	273.07	4.037	39.48	0.43	1.1	0.87	0.9	40	273.05	19.490	268.43	0.98	0.4	0.62	0.2
10	273.06	4.568	45.89	0.45	1.0	0.85	0.8	41	273.06	19.898	271.74	0.87	0.3	0.62	0.1
11	273.02	5.020	51.69	0.46	0.9	0.83	0.7	42	273.05	20.545	276.64	0.71	0.3	0.63	0.1
12	273.04	5.526	58.55	0.48	0.8	0.80	0.7	43	273.07	21.088	280.47	0.60	0.2	0.64	0.1
13	273.05	6.060	66.20	0.49	0.7	0.78	0.6	44	273.08	21.490	283.16	0.52	0.2	0.64	0.1
14	273.05	6.535	73.36	0.49	0.7	0.76	0.5	45	273.07	22.026	286.58	0.44	0.2	0.65	0.1
15	273.06	7.007	80.78	0.51	0.6	0.74	0.5	46	273.10	22.561	289.86	0.37	0.1	0.66	0.1
16	273.06	7.503	88.86	0.52	0.6	0.72	0.4	47	273.11	23.102	293.06	0.36	0.1	0.67	0.1
17	273.08	8.037	97.86	0.54	0.5	0.70	0.4	48	273.12	23.507	295.40	0.34	0.1	0.68	0.1
18	273.09	8.509	106.04	0.55	0.5	0.68	0.4	49	273.13	24.081	298.69	0.32	0.1	0.69	0.1
19	273.09	8.697	109.34	0.56	0.5	0.68	0.3	50	273.14	24.511	301.13	0.31	0.1	0.69	0.1
20	273.11	9.417	122.17	0.58	0.5	0.66	0.3	51	273.15	25.182	304.96	0.29	0.1	0.70	0.1
21	273.11	10.159	135.60	0.61	0.5	0.64	0.3	52	273.15	25.661	307.41	0.28	0.1	0.71	0.1
22	273.14	10.580	143.25	0.63	0.4	0.63	0.3	53	273.14	26.076	309.49	0.27	0.1	0.72	0.1
23	273.13	10.896	148.97	0.65	0.4	0.62	0.3	54	273.14	26.577	312.08	0.26	0.1	0.72	0.1
24	273.13	11.490	159.68	0.68	0.4	0.61	0.3	55	273.14	26.982	314.11	0.25	0.1	0.73	0.1
25	273.13	12.024	169.16	0.70	0.4	0.60	0.3	56	273.13	27.492	316.71	0.24	0.1	0.74	0.1
26	273.17	12.519	177.81	0.73	0.4	0.60	0.2	57	273.13	28.026	319.37	0.23	0.1	0.75	0.1
27	273.16	13.305	191.11	0.77	0.4	0.59	0.2	58	273.13	28.568	321.92	0.22	0.1	0.75	0.1
28	273.13	13.513	194.52	0.79	0.4	0.59	0.2	59	273.13	29.088	324.13	0.22	0.1	0.76	0.1
29	273.13	14.007	202.45	0.82	0.4	0.59	0.2	60	273.13	29.546	325.75	0.21	0.1	0.77	0.1
30	273.11	14.299	207.01	0.83	0.4	0.59	0.2	61	273.13	29.999	327.01	0.21	0.1	0.78	0.1
31	273.13	14.904	216.11	0.87	0.4	0.59	0.2								

Table 11 – Experimental results of the 0.8197 mole CH_4 + 0.1803 mole H_2S system at 293K, $u(x_{H2S})$= 0.0008, u(T)= 0.03 K, u(P)= 0.003 MPa for pressures up to 5 MPa and u(P)= 0.005 MPa for pressures from 5 to 30 MPa.

No	T [K]	P [MPa]	ρ $\left[\dfrac{kg}{m^3}\right]$	u(ρ) $\left[\dfrac{kg}{m^3}\right]$	u(ρ) %	Z	u(Z) 10^{-2}	No	T [K]	P [MPa]	ρ $\left[\dfrac{kg}{m^3}\right]$	u(ρ) $\left[\dfrac{kg}{m^3}\right]$	u(ρ) %	Z	u(Z) 10^{-2}
1	293.27	0.193	1.54	0.15	9.7	0.99	9.5	32	293.45	15.532	182.32	0.84	0.5	0.67	0.3
2	293.27	0.498	4.03	0.21	5.2	0.98	5.1	33	293.41	16.017	188.26	0.87	0.5	0.67	0.3
3	293.35	0.936	7.74	0.23	3.0	0.96	2.9	34	293.45	16.485	193.92	0.90	0.5	0.67	0.2
4	293.33	1.434	12.03	0.27	2.2	0.94	2.1	35	293.40	17.009	200.00	0.94	0.5	0.67	0.2
5	293.36	1.962	16.56	0.30	1.8	0.94	1.6	36	293.41	17.526	205.67	0.97	0.5	0.67	0.2
6	293.35	2.422	20.50	0.33	1.6	0.93	1.4	37	293.42	18.033	211.20	1.01	0.5	0.68	0.2
7	293.38	2.915	26.63	0.36	1.4	0.87	1.1	38	293.42	18.536	216.41	1.02	0.5	0.68	0.2
8	293.33	3.440	30.85	0.38	1.2	0.88	1.0	39	293.41	19.019	221.14	0.92	0.4	0.68	0.2
9	293.42	3.941	35.88	0.40	1.1	0.87	1.0	40	293.41	19.519	225.91	0.79	0.4	0.68	0.2
10	293.35	4.502	41.72	0.43	1.0	0.85	0.9	41	293.41	20.054	230.93	0.65	0.3	0.69	0.1
11	293.32	5.019	46.91	0.44	0.9	0.85	0.8	42	293.42	20.511	234.95	0.54	0.2	0.69	0.1
12	293.32	5.508	52.59	0.45	0.9	0.83	0.8	43	293.41	21.059	239.83	0.40	0.2	0.69	0.1
13	293.34	6.006	58.11	0.46	0.8	0.82	0.6	44	293.35	21.512	243.53	0.39	0.2	0.70	0.1
14	293.31	6.513	63.51	0.46	0.7	0.81	0.5	45	293.34	22.090	248.06	0.37	0.1	0.70	0.1
15	293.32	7.004	68.50	0.47	0.7	0.81	0.5	46	293.37	22.488	251.05	0.36	0.1	0.71	0.1
16	293.32	7.520	74.89	0.48	0.6	0.79	0.4	47	293.39	22.971	254.58	0.34	0.1	0.71	0.1
17	293.33	8.008	80.89	0.49	0.6	0.78	0.4	48	293.41	23.490	258.21	0.32	0.1	0.72	0.1
18	293.32	8.507	87.23	0.51	0.6	0.77	0.4	49	293.39	24.024	261.83	0.31	0.1	0.73	0.1
19	293.33	9.072	94.80	0.53	0.6	0.76	0.4	50	293.39	24.659	266.01	0.29	0.1	0.73	0.1
20	293.32	9.526	100.87	0.54	0.5	0.75	0.3	51	293.42	25.034	268.44	0.28	0.1	0.74	0.1
21	293.37	10.013	107.38	0.56	0.5	0.74	0.3	52	293.41	25.538	271.56	0.27	0.1	0.74	0.1
22	293.32	10.518	114.24	0.58	0.5	0.73	0.3	53	293.37	26.028	274.53	0.26	0.1	0.75	0.1
23	293.33	10.922	121.63	0.60	0.5	0.71	0.3	54	293.42	26.523	277.36	0.25	0.1	0.76	0.1
24	293.35	11.685	130.63	0.63	0.5	0.71	0.3	55	293.41	27.022	280.18	0.24	0.1	0.76	0.1
25	293.36	12.068	136.11	0.65	0.5	0.70	0.3	56	293.37	27.520	283.00	0.23	0.1	0.77	0.1
26	293.36	12.506	142.15	0.67	0.5	0.70	0.3	57	293.38	27.986	285.56	0.22	0.1	0.78	0.1
27	293.36	13.036	149.41	0.70	0.5	0.69	0.3	58	293.38	28.437	287.96	0.21	0.1	0.78	0.1
28	293.36	13.500	155.72	0.72	0.5	0.69	0.3	59	293.38	28.979	290.66	0.21	0.1	0.79	0.1
29	293.34	14.027	162.75	0.75	0.5	0.68	0.3	60	293.37	29.405	292.65	0.20	0.1	0.80	0.1
30	293.34	14.501	169.12	0.78	0.5	0.68	0.3	61	293.37	29.932	295.13	0.20	0.1	0.80	0.1
31	293.37	15.006	175.59	0.81	0.5	0.68	0.3								

Table 12 – Experimental results of the 0.714 mole CH$_4$ + 0.286 mole H$_2$S system at 253K, u(x$_{H2S}$)= 0.0011, u(T)= 0.03 K, u(P)= 0.003 MPa for pressures up to 5 MPa and u(P)= 0.005 MPa for pressures from 5 to 30 MPa.

No	T	P	ρ	u(ρ)		Z	u(Z)	No	T	P	ρ	u(ρ)		Z	u(Z)
	[K]	[MPa]	$\left[\dfrac{kg}{m^3}\right]$	$\left[\dfrac{kg}{m^3}\right]$	%		10^{-2}		[K]	[MPa]	$\left[\dfrac{kg}{m^3}\right]$	$\left[\dfrac{kg}{m^3}\right]$	%		10^{-2}
1	252.96	0.508	5.18	0.23	4.4	0.99	4.3	21	253.11	20.550	389.58	0.89	0.2	0.53	0.1
2	252.94	1.010	10.45	0.30	2.9	0.97	2.7	22	253.10	21.049	391.70	0.85	0.2	0.54	0.1
3	252.95	1.513	16.11	0.37	2.3	0.95	2.2	23	253.15	21.583	393.97	0.80	0.2	0.55	0.1
4	253.00	2.008	22.87	0.43	1.9	0.88	1.7	24	253.17	22.039	395.89	0.76	0.2	0.56	0.1
5	253.02	2.407	28.16	0.48	1.7	0.86	1.5	25	253.15	22.523	397.90	0.73	0.2	0.57	0.1
6	253.27	13.000	342.99	1.03	0.3	0.38	0.2	26	253.09	23.043	399.91	0.69	0.2	0.58	0.1
7	253.23	13.535	348.43	1.07	0.3	0.39	0.2	27	253.07	23.585	402.01	0.66	0.2	0.59	0.1
8	253.17	14.005	352.44	1.11	0.3	0.40	0.2	28	253.09	24.033	403.73	0.63	0.2	0.60	0.1
9	253.25	14.514	356.43	1.15	0.3	0.41	0.2	29	253.12	24.495	405.58	0.60	0.1	0.61	0.1
10	253.16	15.038	360.04	1.20	0.3	0.42	0.2	30	253.14	25.004	407.49	0.58	0.1	0.62	0.1
11	253.22	15.498	363.19	1.25	0.3	0.43	0.2	31	253.11	25.528	409.34	0.55	0.1	0.63	0.1
12	253.14	16.004	366.38	1.29	0.4	0.44	0.3	32	253.09	25.963	410.91	0.54	0.1	0.64	0.1
13	253.21	16.513	369.43	1.34	0.4	0.45	0.3	33	253.06	26.459	412.74	0.52	0.1	0.65	0.1
14	253.18	17.054	372.46	1.27	0.3	0.46	0.2	34	253.05	26.980	414.51	0.50	0.1	0.66	0.1
15	253.13	17.511	374.95	1.22	0.3	0.47	0.2	35	253.07	27.494	416.29	0.49	0.1	0.67	0.1
16	253.19	18.047	377.75	1.15	0.3	0.48	0.2	36	253.10	28.034	418.14	0.48	0.1	0.68	0.1
17	253.16	18.491	380.05	1.10	0.3	0.49	0.2	37	253.13	28.568	420.00	0.47	0.1	0.69	0.1
18	253.12	19.058	382.70	1.04	0.3	0.50	0.2	38	253.16	29.087	421.82	0.46	0.1	0.69	0.1
19	253.15	19.521	384.91	0.99	0.3	0.51	0.2	39	253.16	29.450	423.08	0.46	0.1	0.70	0.1
20	253.16	20.070	387.42	0.94	0.2	0.52	0.1	40	253.16	30.025	425.02	0.46	0.1	0.71	0.1

Table 13 – Experimental results of the 0.714 mole CH$_4$ + 0.286 mole H$_2$S system at 273K, u(x$_{H2S}$)= 0.0011, u(T)= 0.03 K, u(P)= 0.003 MPa for pressures up to 5 MPa and u(P)= 0.005 MPa for pressures from 5 to 30 MPa.

No	T	P	ρ	u(ρ)		Z	u(Z)	No	T	P	ρ	u(ρ)		Z	u(Z)
	[K]	[MPa]	$\left[\dfrac{kg}{m^3}\right]$	$\left[\dfrac{kg}{m^3}\right]$	%		10^{-2}		[K]	[MPa]	$\left[\dfrac{kg}{m^3}\right]$	$\left[\dfrac{kg}{m^3}\right]$	%		10^{-2}
1	272.97	0.448	4.32	0.22	5.1	0.97	5.0	25	273.10	18.931	331.97	1.16	0.3	0.53	0.2
2	272.98	0.925	9.10	0.25	2.7	0.95	2.5	26	273.16	19.608	336.94	0.94	0.3	0.54	0.2
3	272.99	1.499	15.62	0.29	1.8	0.89	1.6	27	273.23	20.100	340.42	0.81	0.2	0.55	0.1
4	272.98	1.959	21.08	0.32	1.5	0.86	1.4	28	273.20	20.623	344.02	0.69	0.2	0.56	0.1
5	272.99	2.470	27.39	0.35	1.3	0.84	1.2	29	273.19	21.199	347.78	0.57	0.2	0.57	0.1
6	273.07	2.991	34.29	0.38	1.1	0.81	1.0	30	273.21	21.506	349.84	0.52	0.1	0.57	0.1
7	273.06	3.515	41.26	0.41	1.0	0.80	0.9	31	273.14	21.825	351.99	0.47	0.1	0.58	0.1
8	273.02	4.006	49.21	0.43	0.9	0.76	0.7	32	273.16	22.152	354.18	0.42	0.1	0.58	0.1
9	273.02	4.495	57.70	0.45	0.8	0.73	0.6	33	273.16	22.483	356.27	0.38	0.1	0.59	0.1
10	273.00	5.009	66.37	0.46	0.7	0.71	0.6	34	273.18	22.828	358.14	0.37	0.1	0.60	0.1
11	273.03	5.418	73.50	0.47	0.6	0.69	0.5	35	273.20	23.590	362.19	0.34	0.1	0.61	0.1
12	273.01	12.511	252.68	0.73	0.3	0.46	0.2	36	273.37	24.085	364.70	0.32	0.1	0.62	0.1
13	273.00	13.055	265.48	0.76	0.3	0.46	0.2	37	273.25	24.591	367.01	0.31	0.1	0.63	0.1
14	273.00	13.551	273.70	0.79	0.3	0.46	0.2	38	273.19	24.981	368.95	0.30	0.1	0.63	0.1
15	273.00	14.019	280.64	0.82	0.3	0.47	0.2	39	273.23	25.533	371.48	0.28	0.1	0.64	0.1
16	273.00	14.532	287.50	0.85	0.3	0.47	0.2	40	273.25	26.031	373.67	0.27	0.1	0.65	0.1
17	273.01	14.977	293.17	0.88	0.3	0.48	0.2	41	273.22	26.410	375.25	0.26	0.1	0.66	0.1
18	273.00	15.457	298.99	0.91	0.3	0.48	0.2	42	273.24	27.020	377.85	0.25	0.1	0.67	0.1
19	272.99	15.974	304.94	0.95	0.3	0.49	0.2	43	273.05	27.474	379.67	0.24	0.1	0.68	0.1
20	272.99	16.531	310.78	0.98	0.3	0.50	0.2	44	273.06	27.956	381.54	0.23	0.1	0.68	0.1
21	273.03	16.977	315.19	1.02	0.3	0.50	0.2	45	273.10	28.471	383.53	0.23	0.1	0.69	0.1
22	273.08	17.450	319.61	1.05	0.3	0.51	0.2	46	273.05	29.015	385.58	0.22	0.1	0.70	0.1
23	273.11	17.956	324.07	1.09	0.3	0.52	0.2	47	273.03	29.571	387.72	0.21	0.1	0.71	0.1
24	273.09	18.521	328.70	1.13	0.3	0.53	0.2	48	273.03	30.070	389.49	0.21	0.1	0.72	0.1

Table 14 – Experimental results of the 0.714 mole CH_4 + 0.286 mole H_2S system at 293K, $u(x_{H2S})$= 0.0011, $u(T)$= 0.03 K, $u(P)$= 0.003 MPa for pressures up to 5 MPa and $u(P)$= 0.005 MPa for pressures from 5 to 30 MPa.

No	T	P	ρ	u(ρ)		Z	u(Z)	No	T	P	ρ	u(ρ)		Z	u(Z)
	[K]	[MPa]	$\left[\frac{kg}{m^3}\right]$	$\left[\frac{kg}{m^3}\right]$	%		10^{-2}		[K]	[MPa]	$\left[\frac{kg}{m^3}\right]$	$\left[\frac{kg}{m^3}\right]$	%		10^{-2}
1	293.27	0.227	1.99	0.19	9.5	0.99	9.3	34	293.30	15.503	239.94	0.84	0.4	0.56	0.3
2	293.27	0.560	4.92	0.21	4.3	0.99	4.2	35	293.31	16.108	249.28	0.88	0.4	0.56	0.3
3	293.28	1.101	9.72	0.25	2.6	0.98	2.5	36	293.34	16.524	253.44	0.91	0.4	0.57	0.3
4	293.28	1.547	14.1	0.29	2.1	0.95	2.0	37	293.34	17.035	260.09	0.94	0.4	0.57	0.3
5	293.28	2.065	19.16	0.31	1.6	0.94	1.5	38	293.35	17.740	267.95	0.99	0.4	0.57	0.3
6	293.30	2.511	23.63	0.34	1.4	0.92	1.2	39	293.33	18.012	271.26	1.00	0.4	0.58	0.3
7	293.29	2.976	28.53	0.37	1.3	0.91	1.1	40	293.33	18.543	276.99	1.02	0.4	0.58	0.3
8	293.29	3.489	33.95	0.40	1.2	0.89	1.0	41	293.33	19.012	281.75	0.92	0.3	0.59	0.2
9	293.42	3.851	38.01	0.41	1.1	0.88	1.0	42	293.33	19.476	286.23	0.80	0.3	0.59	0.2
10	293.43	4.386	46.59	0.42	0.9	0.82	0.8	43	293.34	20.081	291.58	0.65	0.2	0.60	0.1
11	293.44	4.823	51.27	0.43	0.8	0.82	0.7	44	293.34	20.504	295.67	0.54	0.2	0.60	0.1
12	293.39	5.407	58.83	0.45	0.8	0.80	0.7	45	293.31	21.026	300.53	0.41	0.1	0.61	0.1
13	293.32	5.943	66.82	0.46	0.7	0.77	0.6	46	293.33	21.863	306.80	0.38	0.1	0.62	0.1
14	293.33	6.464	75.29	0.46	0.6	0.75	0.4	47	293.32	22.053	308.34	0.37	0.1	0.62	0.1
15	293.31	6.885	80.49	0.47	0.6	0.74	0.4	48	293.31	22.118	308.67	0.37	0.1	0.62	0.1
16	293.27	7.261	85.92	0.48	0.6	0.74	0.4	49	293.31	22.512	311.24	0.36	0.1	0.63	0.1
17	293.27	7.749	94.83	0.49	0.5	0.71	0.4	50	293.30	22.979	314.55	0.34	0.1	0.64	0.1
18	293.28	8.092	103.64	0.50	0.5	0.68	0.4	51	293.30	23.460	317.83	0.32	0.1	0.64	0.1
19	293.29	8.523	108.80	0.51	0.5	0.68	0.4	52	293.31	23.712	319.93	0.32	0.1	0.64	0.1
20	293.30	9.149	119.96	0.53	0.4	0.66	0.3	53	293.29	23.988	321.16	0.31	0.1	0.65	0.1
21	293.30	9.741	129.36	0.55	0.4	0.66	0.3	54	293.30	24.512	324.48	0.29	0.1	0.66	0.1
22	293.33	10.169	136.99	0.57	0.4	0.65	0.3	55	293.29	25.012	327.50	0.28	0.1	0.66	0.1
23	293.29	10.516	145.41	0.58	0.4	0.63	0.3	56	293.30	25.515	330.43	0.27	0.1	0.67	0.1
24	293.29	11.236	161.66	0.61	0.4	0.60	0.3	57	293.30	25.988	333.07	0.26	0.1	0.68	0.1
25	293.30	11.789	174.33	0.64	0.4	0.59	0.3	58	293.31	26.506	335.86	0.24	0.1	0.69	0.1
26	293.32	12.220	183.56	0.66	0.4	0.58	0.3	59	293.33	26.879	337.31	0.24	0.1	0.69	0.1
27	293.32	12.521	189.88	0.67	0.4	0.57	0.3	60	293.64	27.145	339.08	0.23	0.1	0.70	0.1
28	293.31	12.964	198.31	0.69	0.4	0.57	0.3	61	293.53	27.520	340.85	0.23	0.1	0.70	0.1
29	293.30	13.528	208.17	0.72	0.3	0.57	0.2	62	293.43	28.085	343.33	0.22	0.1	0.71	0.1
30	293.29	13.780	213.21	0.74	0.3	0.56	0.2	63	293.42	28.586	345.52	0.21	0.1	0.72	0.1
31	293.30	14.426	223.09	0.78	0.3	0.56	0.2	64	293.40	29.019	347.54	0.21	0.1	0.73	0.1
32	293.31	14.523	224.65	0.78	0.3	0.56	0.2	65	293.33	29.517	349.82	0.20	0.1	0.73	0.1
33	293.30	15.049	233.30	0.81	0.3	0.56	0.2	66	293.33	29.998	352.02	0.20	0.1	0.74	0.1

Table 15 - Absolute average deviations (%AAD) between the studied models and the densities measured in this work.

x_{H2S}	T/K	SAFT-VR Mie	PR	GERG 2008
x=0.1315	253	3.3	4.8	2.1
	273	1.6	1.4	2.0
	293	3.9	2.2	4.3
	Total	3.0	2.9	2.8
x=0.1801	253	1.6	3.4	2.5
	273	1.5	2.0	2.6
	293	2.5	2.0	3.3
	Total	1.9	2.5	2.8
x=0.2860	253	1.8	4.1	4.6
	273	3.2	3.8	5.3
	293	3.1	3.1	4.8
	Total	2.8	3.6	4.9

Table 16 – Absolute average deviation (%AAD) between the available experimental data and the studied models.

Author	No Data	PR	PR+Peneloux	SAFT-VR Mie	GERG 2008
Bailey et al.	80	5.1	3.9	4.6	3.3
Reamer et al.	1140	10.2	5.5	5.0	5.3
This work	526	3.0	5.2	2.5	3.4
Total	1748	7.8	5.4	4.3	4.6

Table 17 – Regressed parameters for the calculation of the second virial coefficient *B*, condition ranges and AAD deviations between the correlation and experimental compressibility factors.

Parameters	a ($m^3 \cdot mol^{-1}$)	b ($m^3 \cdot K \cdot mol^{-1}$)	c ($m^3 \cdot K^3 \cdot mol^{-1}$)	d ($m^3 \cdot mol^{-1}$)
	1.5385×10^{-4}	-6.6201×10^{-2}	-1.5017×10^2	9.1010×10^{-5}

Range	CH_4 mole fraction	Pressure (MPa)	Temperature (K)
	0.1 - 0.9	0.17 – 1.88	253 - 500

Deviation	%AAD	Max.Dev.
	1.5%	5.7%
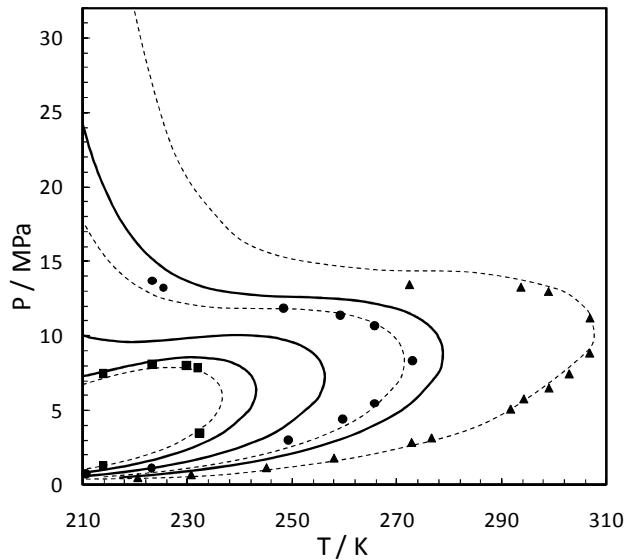
Figure 1. Predicted phases envelopes with the PR EoS of the methane + hydrogen sulphide system with 0.1101, 0.1315, 0.1803, 0.248, 0.286 and 0.458 mol fractions of H$_2$S. The solid lines are the compositions studied in this work and the dashe lines are other phase diagrams compared against Kohn and Kurata data [22]: (■) 0.1101, (●) 0.248 and (▲) 0.458 mol fractions of H$_2$S.
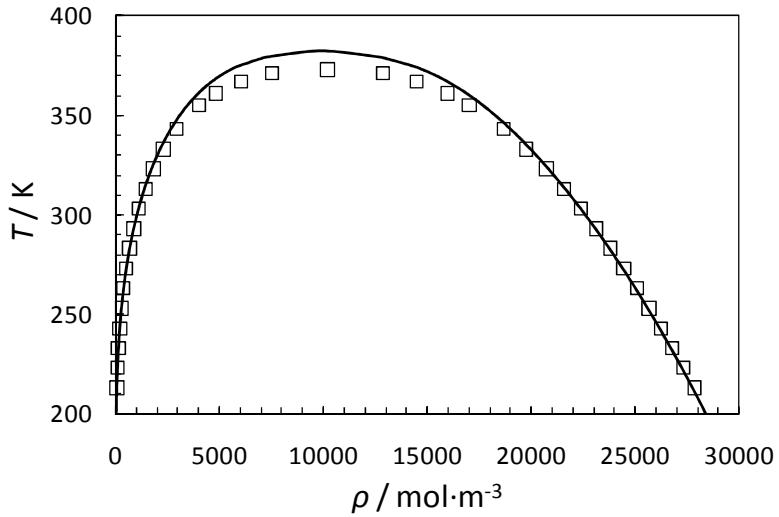
Figure 2. Temperature-density coexistence envelop for pure H$_2$S. Comparison between experimental data (□) [32] and SAFT-VR Mie calculation.
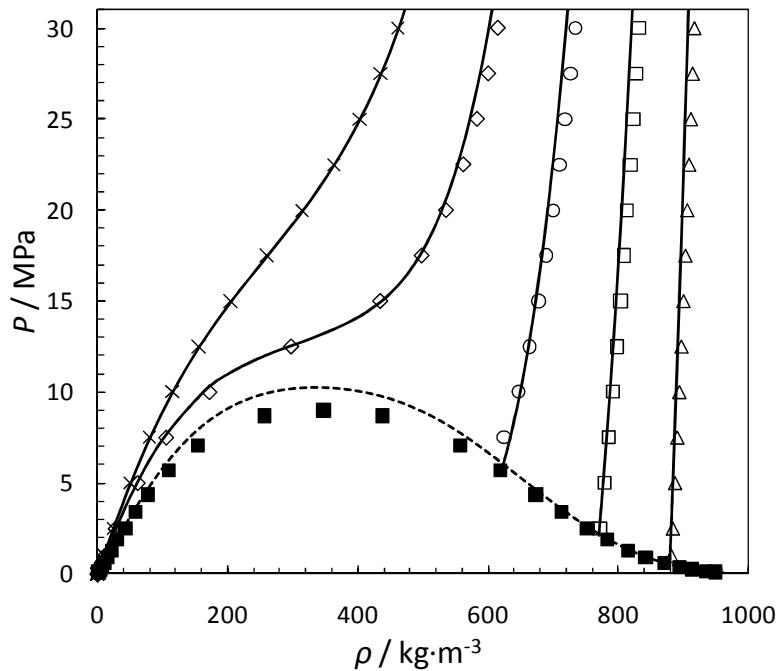
Figure 3. Predicted and experimental densities of pure H$_2$S. The solid lines are isotherms calculated with the SAFT-VR Mie and the dashed line is the calculated coexistence curve. The symbols denote experimental data: from the literature [32] at T=250K (Δ), T=300K (□), T=350K (○), T=400K (◇) and T=450K (×) and at saturation (■).
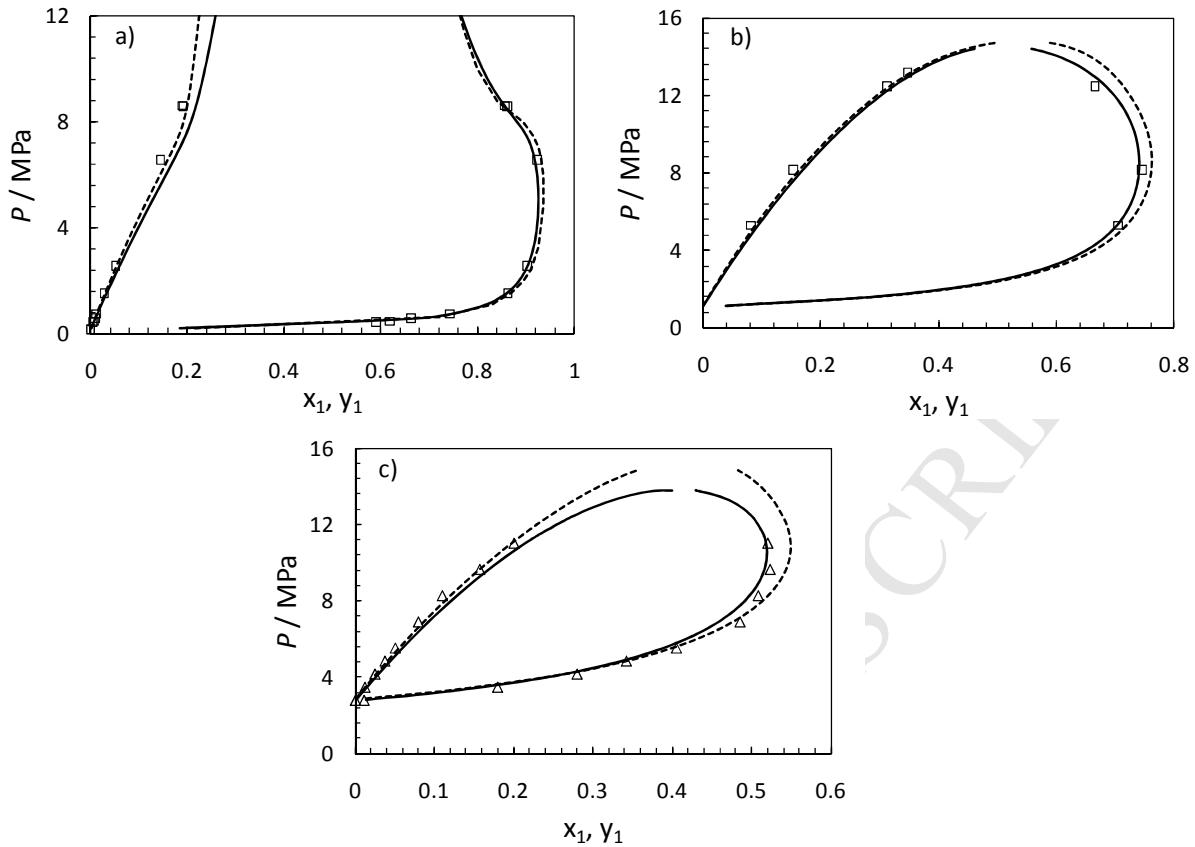
Figure 4. P-x diagrams of CH$_4$ (1) + H$_2$S (2) system at a) T =223.17K, b) T =273.54K and c) T=310.93. Symbols: (□) Coquelet et al. [7] and (△) Kohn and Kurata [22]. Solid line: calculated bubble and dew lines using PR model with k$_{ij}$ = 0.0807. Dashed line: calculated bubble and dew lines using SAFT-VR Mie EoS with k$_{ij}$ = 0.0314.
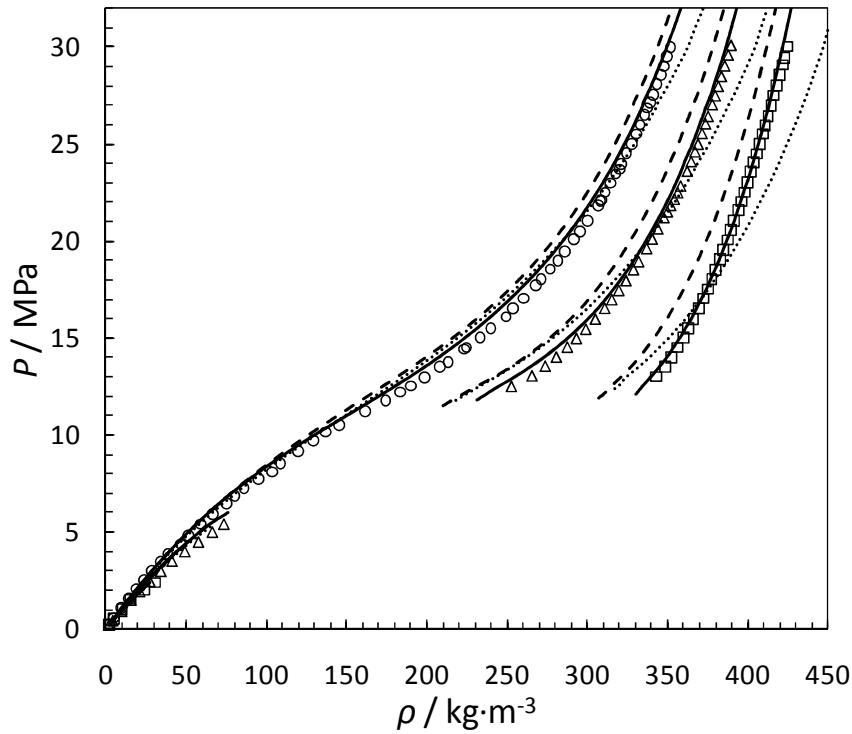
Figure 5. Experimental and predicted densities of the 0.714 mole CH$_2$ + 0.286 mole H$_2$S system. Experimental results: (□) 253 K, (○) 273 K, (△) 293 K. Lines: Predictions using the SAFT-VR Mie EoS. Dashed lines: Predictions using the GERG-2008 EoS. Dotted lines: Predictions using the PR EoS.
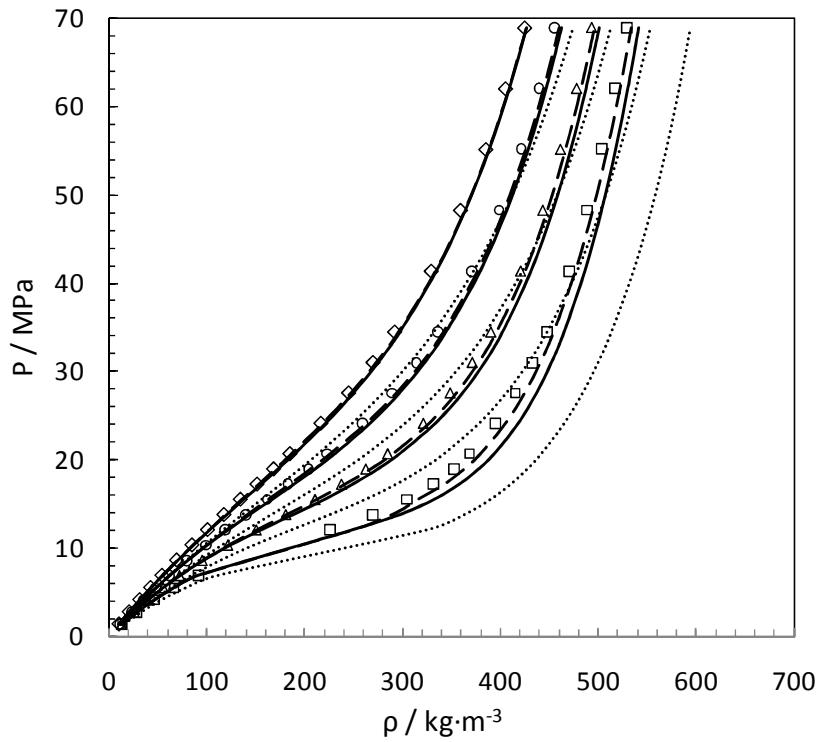
Figure 6. Experimental and predicted densities of the 0.5 mole CH$_4$ + 0.5 mole H$_2$S system. Experimental results: (□) 311 K, (△) 344 K, (○) 377 K and (◇) 411 K [8]. Lines: Predictions using the SAFT-VR Mie EoS. Dashed lines: Predictions using the GERG-2008 EoS. Dotted lines: Predictions using the PR+Peneloux EoS.
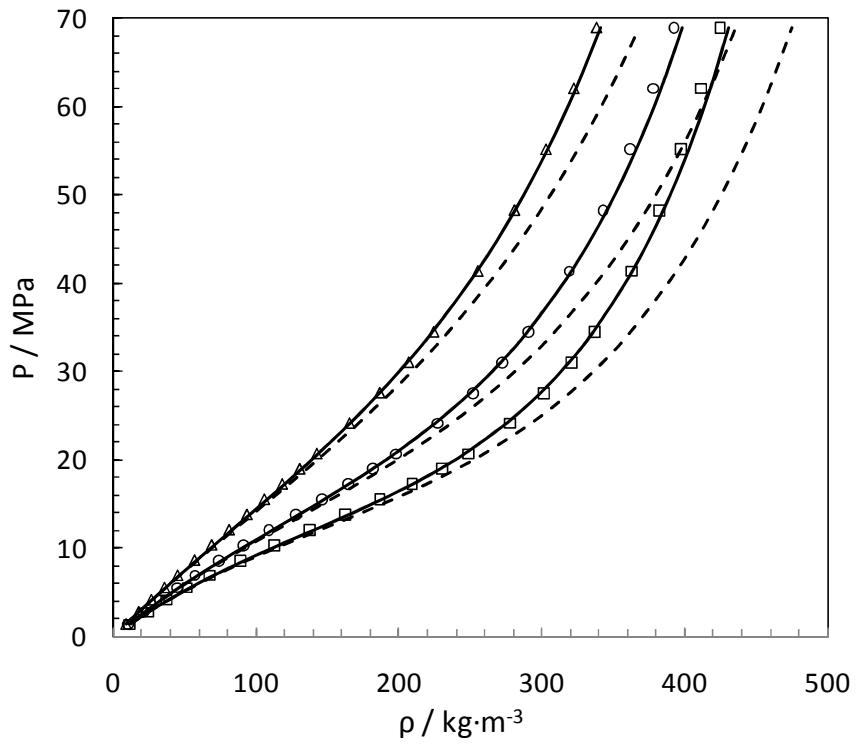
Figure 7. Experimental and predicted densities of the 0.7 mole CH$_4$ + 0.3 mole H$_2$S system. Comparison of PR+Peneloux (continuous curve), PR (dashes) and literature data at T=311K (□), T=344K (○) and T=411K (△) [8]**.**
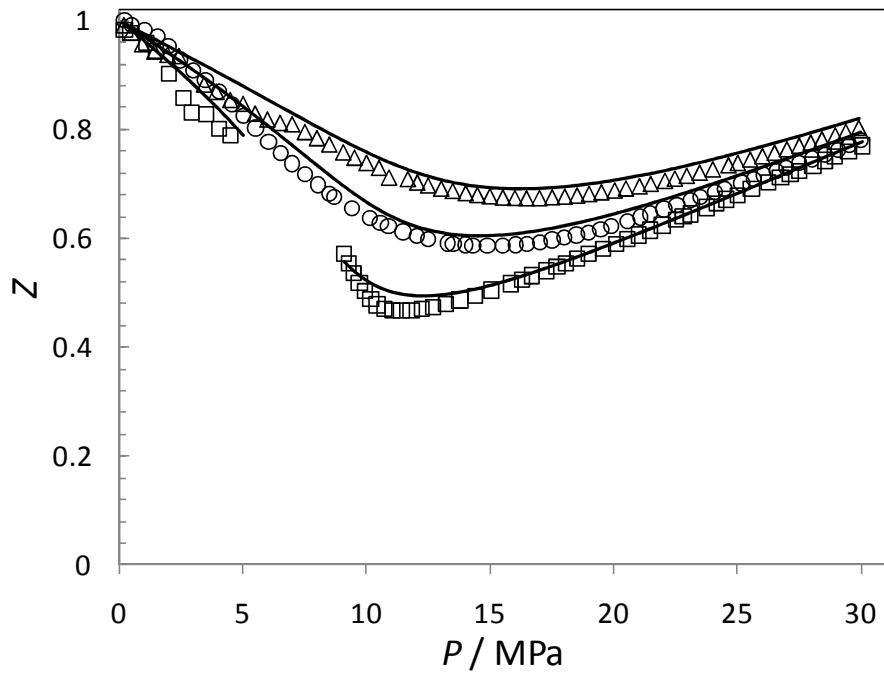
Figure 8. Compressibility factor of the 0.8197 mol CH$_4$ + 0.1803 mol H$_2$S system. Comparison betwen the SAFT-VR Mie calculation and experimental data measured in this work: T=253K (□), T=273K (○) and T=293K (△).
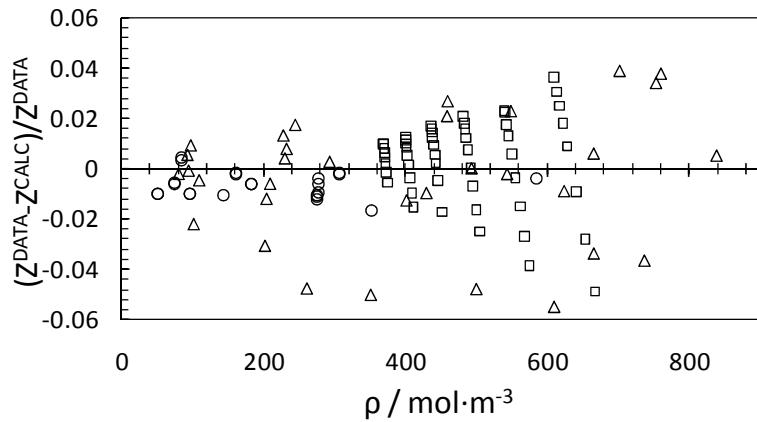
Figure 9. Deviations between this work (△), Reamer et al. data (□) [8] and Bailey et al. data (○) [10] and predictions using low pressure virial EoS from
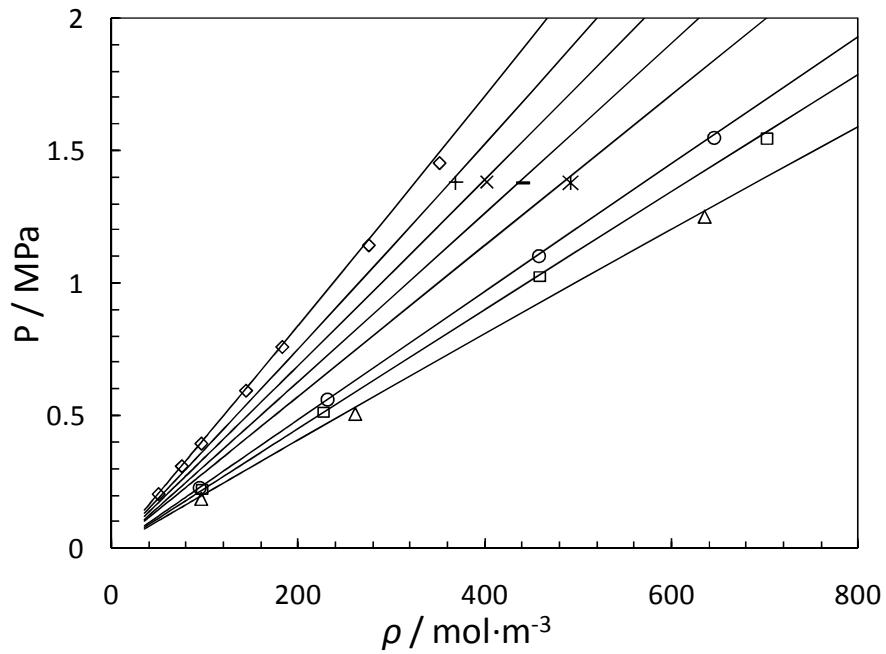
Figure 10. P-ρ diagram of several systems of H_2S + CH_4 at 8 isotherms. Comparison of predictions with low pressure virial EoS and experimental data: T=253K and x_{CH4}=0.87 ($\triangle$), T=273K and x_{CH4}=0.82 ($\square$), T=293K and x_{CH4}=0.71 ($\bigcirc$), T=344K and x_{CH4}=0.4 ($*$), T=377K and x_{CH4}=0.5 ($-$), T=411K and x_{CH4}=0.6 (+), T=444K and x_{CH4}=0.8 ($\times$) and T=500K and x_{CH4}=0.5 ($\diamond$) [8] [10].

References

[1] Energy.ihs.com, "EDIN database, fields and reservoir information," 2009.

[2] W. F. J. Burgers, P. S. Northrop, H. S. Kheshgi, and J. A. Valencia, "Worldwide development potential for sour gas," *Energy Procedia*, vol. 4, pp. 2178–2184, 2011.

[3] N. W. Chakroun and A. F. Ghoniem, "High-efficiency low LCOE combined cycles for sour gas oxy-combustion with CO2 capture," *Int. J. Greenh. Gas Control*, vol. 41, pp. 1–11, 2015.

[4] M. E. Boot-Handford, J. C. Abanades, E. J. Anthony, M. J. Blunt, S. Brandani, N. Mac Dowell, and J. R. Fernandez, "Carbon capture and storage update," *Energy Environ. Sci.*, vol. 7, no. 1, pp. 130–189, 2014.

[5] H. H. Reamer, B. H. Sage, and W. N. Lacey, "Volumetric Behavior of Hydrogen Sulfide," *Ind. Eng. Chem.*, vol. 42, no. 1, pp. 140–143, Jan. 1950.

[6] P. Mougin, X. Renaud, and G. Elbaz, "Operational validation of the Sprex process for bulk H2S and mercaptans removal," *Gas Ind Curr Futur.*, no. 6, pp. 17–19, 2008.

[7] C. Coquelet, A. Valtz, P. Stringari, M. Popovic, D. Richon, and P. Mougin, "Phase equilibrium data for the hydrogen sulphide+methane system at temperatures from 186 to 313K and pressures up to about 14MPa," *Fluid Phase Equilib.*, vol. 383, pp. 94–99, Dec. 2014.

[8] H. H. Reamer, B. H. Sage, and W. N. Lacey, "Phase Equilibria in Hydrocarbon Systems - Volumetric and Phase Behavior of the Methane-Hydrogen Sulfide System," *Ind. Eng. Chem.*, vol. 43, no. 4, pp. 976–981, Apr. 1951.

[9] N. Sakoda and M. Uematsu, "A Thermodynamic Property Model for the Binary Mixture of Methane and Hydrogen Sulfide," *Int. J. Thermophys.*, vol. 26, no. 5, pp. 1303–1325, Sep. 2005.

[10] D. M. Bailey, C. H. Liu, J. C. Holste, and K. R. Hall, "Gas Processors Assoc. Research Report 107, Tulsa, Oklahoma," 1987.

[11] D. Y. Peng and D. B. Robinson, "A New Two-Constant Equation of State," *Ind. Eng. Chem. Fundam.*, vol. 15, no. 1, pp. 59–64, Feb. 1976.

[12] T. Lafitte, A. Apostolakou, C. Avendaño, A. Galindo, C. S. Adjiman, E. a Müller, and G. Jackson, "Accurate statistical associating fluid theory for chain molecules formed from Mie segments.," *J. Chem. Phys.*, vol. 139, no. 15, p. 154504, Oct. 2013.

[13] O. Kunz and W. Wagner, "The GERG-2008 wide-range equation of state for natural gases and other mixtures: An expansion of GERG-2004," *J. Chem. Eng. Data*, vol. 57, no. 11, pp. 3032–3091, 2012.

[14] C. Bouchot and D. Richon, "An enhanced method to calibrate vibrating tube densimeters," *Fluid Phase Equilib.*, vol. 191, pp. 189–208, 2001.

[15] C. Coquelet, D. Ramjugernath, H. Madani, A. Valtz, P. Naidoo, and A. H. Meniai,

"Experimental measurement of vapor pressures and densities of pure hexafluoropropylene," *J. Chem. Eng. Data*, vol. 55, no. 6, pp. 2093–2099, 2010.

[16] M. Nazeri, A. Chapoy, A. Valtz, C. Coquelet, and B. Tohidi, "Densities and derived thermophysical properties of the 0.9505 CO_2+0.0495 H_2S mixture from 273 K to 353 K and pressures up to 41 MPa," *Fluid Phase Equilib.*, vol. 423, pp. 156–171, 2016.

[17] C. Coquelet and D. Richon, "Experimental determination of phase diagram and modeling : Application to refrigerant mixtures ´ rmination expe ´ rimentale des diagrammes de phases et De ´ lisations : Application aux me ´ langes de fluides leurs mode ` nes frigorige," *Int. J. Refrig.*, vol. 32, no. 7, pp. 1604–1614, 2009.

[18] "JCGM 200: 2012 International vocabulary of metrology – Basic and general concepts and associated terms (VIM)," no. Vim, 2012.

[19] B. N. T. and C. E. Kuyatt, "NIST Technical Note 1297. Edition Guidelines for Evaluating and Expressing the Uncertainty of NIST Measurement Results," 1994.

[20] H. H. Ku, "Notes on the use of propagation of error formulas," *J. Res. Natl. Bur. Stand. Sect. C Eng. Instrum.*, vol. 70C, no. 4, p. 263, Oct. 1966.

[21] H. Lin, "Peng-Robinson equation of state for vapor-liquid equilibrium calculations for carbon dioxide + hydrocarbon mixtures," *Fluid Phase Equilib.*, vol. 16, no. 2, pp. 151–169, Jan. 1984.

[22] J. P. Kohn and F. Kurata, "Heterogeneous phase equilibria of the methane—hydrogen sulfide system," *AIChE J.*, vol. 4, no. 2, pp. 211–217, Jun. 1958.

[23] J. O. Valderrama and M. Alfaro, "Liquid volumes from generalized cubic equations of state: Take it with care," *Oil Gas Sci. Technol.*, vol. 55, no. 5, pp. 523–531, 2000.

[24] A. Péneloux, E. Rauzy, and R. Fréze, "A consistent correction for Redlich-Kwong-Soave volumes," *Fluid Phase Equilib.*, vol. 8, no. 1, 1982.

[25] O. Kunz, R. Klimeck, W. Wagner, and M. Jaeschke, *The GERG-2004 Wide-Range Equation of State for Natural Gases and Other Mixtures*. 2007.

[26] A. Chapoy, C. Coquelet, H. Liu, A. Valtz, and B. Tohidi, "Vapour-liquid equilibrium data for the hydrogen sulphide (H_2S)+carbon dioxide (CO_2) system at temperatures from 258 to 313K," *Fluid Phase Equilib.*, vol. 356, pp. 223–228, 2013.

[27] A. Chapoy, H. Haghighi, R. Burgass, and B. Tohidi, "On the phase behaviour of the (carbon dioxide+water) systems at low temperatures: Experimental and modelling," *J. Chem. Thermodyn.*, vol. 47, pp. 6–12, 2012.

[28] H. Haghighi, A. Chapoy, R. Burgess, and B. Tohidi, "Experimental and thermodynamic modelling of systems containing water and ethylene glycol: Application to flow assurance and gas processing," *Fluid Phase Equilib.*, vol. 276, no. 1, pp. 24–30, 2009.

[29] A. Chapoy, M. Nazeri, M. Kapateh, R. Burgass, C. Coquelet, and B. Tohidi, "Effect of impurities on thermophysical properties and phase behaviour of a CO_2-rich system in

CCS," *Int. J. Greenh. Gas Control*, vol. 19, pp. 92–100, 2013.

[30]   R. A. Heidemann and A. M. Khalil, "The calculation of critical points," *AIChE J.*, vol. 26, no. 5, pp. 769–779, Sep. 1980.

[31]   S. Langè, M. Campestrini, and P. Stringari, "Phase behavior of system methane + hydrogen sulfide," *AIChE J.*, vol. 7, no. PART 1, pp. 405–410, May 2016.

[32]   V. Diky, C. D. Muzny, E. W. Lemmon, R. D. Chirico, and M. Frenkel, "NIST Standard Reference Database 103a: NIST ThermoData Engine: Version 2.7 - Pure Compounds," 2007.

[33]   M. Dicko, G. Belaribi-Boukais, C. Coquelet, A. Valtz, F. Brahim Belaribi, P. Naidoo, and D. Ramjugernath, "Experimental measurement of vapor pressures and densities at saturation of pure hexafluoropropylene oxide: Modeling using a crossover equation of state," *Ind. Eng. Chem. Res.*, vol. 50, no. 8, pp. 4761–4768, 2011.

[34]   D. J. Naresh and J. K. Singh, "Virial coefficients of hard-core attractive Yukawa fluids," *Fluid Phase Equilib.*, vol. 285, no. 1–2, pp. 36–43, 2009.